Impact of automated driving systems on road freight transport and electrified propulsion of heavy vehicles

Transportation Research Part C 115 (2020) 102610

Contents lists available at ScienceDirect

Transportation Research Part C

journal homepage: www.elsevier.com/locate/trc

Impact of automated driving systems on road freight transport and electrified propulsion of heavy vehicles

Toheed Ghandriz[a,*], Bengt Jacobson[a], Leo Laine[a,b], Jonas Hellgren[b]

[a] Division of Vehicle Engineering and Autonomous Systems, Department of Mechanics and Maritime Sciences, Chalmers University of Technology, SE-41296 Gothenburg, Sweden

[b] Volvo Group Trucks Technology, SE-40508 Gothenburg, Sweden

ARTICLE INFO

Keywords:
Transportation
Electromobility
Automated driving systems
Heavy vehicles
Electrified propulsion

ABSTRACT

The technological barriers to automated driving systems (ADS) are being quickly overcome to deploy on–road vehicles that do not require a human driver on–board. ADS have opened up possibilities to improve mobility, productivity, logistics planning, and energy consumption. However, further enhancements in productivity and energy consumption are required to reach CO_2–reduction goals, owing to increased demands on transportation. In particular, in the freight sector, incorporation of automation with electrification can meet necessities of sustainable transport. However, the profitability of battery electric heavy vehicles (BEHVs) remains a concern. This study found that ADS led to profitability of BEHVs, which remained profitable for increased travel ranges by a factor of four compared to that of BEHVs driven by humans. Up to 20% reduction in the total cost of ownership of BEHVs equipped with ADS could be achieved by optimizing the electric propulsion system along with the infrastructure for a given transportation task. In that case, the optimized propulsion system might not be similar to that of a BEHV with a human driver. To obtain the results, the total cost of ownership was minimized numerically for 3072 different transportation scenarios that showed the effects of travel distance, road hilliness, average reference speed, and vehicle size on the incorporated electrification and automation, and compared to that of conventional combustion–powered heavy vehicles.

1. Introduction

In the near future, transportation will experience substantial development in the domain of automated driving systems (ADS), which will revolutionize the way people and freight move on-road, as reported by Wadud et al. (2016) and Flämig (2016). Remarkable advantages in terms of user experience, efficiency, safety, mobility, productivity, energy, environment, and economy have been reported with ADS by Alessandrini et al. (2015), Anderson et al. (2014), Brown et al. (2014), Chan (2017), Harper et al. (2016), Levin and Boyles (2015), Maurer et al. (2016), Wadud (2017), Wadud et al. (2016), Taiebat et al. (2018) and Khan et al. (2019), though significant increases in traffic safety due to highly or fully automated vehicles are not certain as revealed by Kalra and Paddock (2016). However, user objectives and motivations differ for passenger cars and freight transport, as reported by Wadud (2017) and Nowakowski et al. (2015). For passenger cars, the major motivations are user experience and environment, whereas in freight transport, as a subject of this study, the most important driving forces are productivity and profitability. For example, increase

* Corresponding author.
E-mail addresses: toheed.ghandriz@chalmers.se (T. Ghandriz), bengt.jacobson@chalmers.se (B. Jacobson), leo.laine@volvo.com (L. Laine), jonas.hellgren@volvo.com (J. Hellgren).

https://doi.org/10.1016/j.trc.2020.102610
Received 17 August 2018; Received in revised form 2 March 2020; Accepted 6 March 2020
Available online 18 March 2020

in the cost of a vehicle related to automation hardware is less important in freight transport, owing to the lower proportion of the automation hardware cost with respect to the total purchase cost, compared to that of passenger cars. Furthermore, ADS permit increased profitability in freight transport, mainly due to a reduction in labor cost as well as due to facilitated logistics and increased utilization and efficiency, as reported by Wadud et al. (2016). Moreover, driver cost reduces significantly in high or full driving automation, resulting in an early adoption of ADS in freight sector.

The reduction in fuel consumption achieved with ADS owing to enhanced vehicle usage and controlled energy management is reported to be only up to 10% in passenger cars, depending on the traffic scenario, compared to that when a human driver is involved, according to Mersky and Samaras (2016). The reduction in fuel consumption achieved with ADS is expected to be higher in freight transport, considering that heavy vehicles can form platoons, which reduce the energy intensity of the following vehicle by up to 25% in theory, according to Wadud et al. (2016), if the gap between vehicles reaches zero; while, measurements showed the average fuel saving of 8% and 15% for 10 m and 4 m gap, respectively, according to Tsugawa et al. (2016). However, as revealed by the European Commission (2016), heavy-duty vehicles contribute to about 25% of the CO_2 emissions from road transport in Europe, which is increasing owing to increasing road freight traffic, despite enhanced fuel consumption efficiency. These figures point to that, despite being a profitable business, the increased efficiency offered by ADS may not result in a reduction in CO_2 emissions in the long term; thus, a further decrease in emissions is required in the transportation sector motivating the development of more environmental-friendly solutions.

In addition to ADS, emerging technologies such as battery electric vehicles can be part of the solution, provided that the electric energy comes from renewable sources. However, the profitability of deploying BEHVs remains a concern in road freight transport. The operating range, payload, weight and volume of goods, charging infrastructure, utilization level, purchase cost, battery life, energy consumption, average speed, available routes, and logistics are among the factors that affect the profitability of BEHVs, according to Wu et al. (2015), Taefi et al. (2016b), Davis and Figliozzi (2013), Feng and Figliozzi (2013), Taefi et al. (2017), Lee et al. (2013), Botsford and Szczepanek (2009), Nesterova et al. (2013), Hovgard et al. (2018), Pelletier et al. (2016), Taefi et al. (2015) and Taefi et al. (2016a). Considering the impacts of high or full driving automation and the requirement of BEHVs profitability, it can be concluded that increased utilization level, enhanced mission planning and logistics, improved energy management, and reduced energy consumption, which can all be achieved with ADS, increase BEHVs profitability and productivity. However, questions remain as to what extent ADS facilitate BEHVs and what the limitations are for different transportation scenarios.

This study, by implementing mathematical optimization and models of vehicle dynamics, showed that the combination of ADS with electrification led to profitability of BEHVs for a wider range of transportation tasks, compared to the case of BEHVs with human drivers. Profitability was determined by evaluating the total cost of ownership (TCO) of BEHVs and compared with that of conventional combustion-powered heavy vehicles (CHVs). To our knowledge, such an incorporation of ADS and freight vehicle electrification was not studied before at the level of details considered in this study that involved the use of a model of vehicle dynamics for different transportation scenarios.

In this study, TCO was considered as an objective function to optimize the vehicle–infrastructure components for different values of vehicle size, distance between charging stations and loading/unloading (LU) points, average speed, and road hilliness that constituted 3072 scenarios. The vehicle–infrastructure components included charging power, LU scheme, the type and size of batteries, the type and number of electric motors, and the size of ICE. Further, analyzing the optimization results based on minimization of the TCO helped to understand the effects of ADS on the optimum propulsion system in both BEHVs and CHVs and showed that the optimum propulsion system might be different for the BEHVs with human drivers and the BEHVs equipped with ADS. Moreover, the transportation tasks where BEHVs become competitive to CHVs with or without ADS were revealed, and it was shown that ADS increase the profitability of BEHVs. It was observed that, in addition to infrastructure, driving cycle and propulsion system, the size of the vehicle exhibited a significant influence on the profitability of BEHVs, therefore, the influence of the size of the vehicle on the profitability was studied in both the cases (vehicles equipped with ADS and those driven by humans). Finally, this research revealed the maximum profit obtained by employing ADS and its dependence on the different transportation tasks and types of vehicles. This study was based on assumptions of the vehicle parameters as well as the components and energy prices, and sensitivity analyses in this regard were carried out, and the results have been reported herein.

In addition, the supplementary material of this paper by Ghandriz et al. (2020) includes the optimization results for all 3072 transportation scenarios, together with the related figures, which allow practitioners to draw their own conclusions on a specific scenario.

This paper is organized as follows. Section 2 provides a short background and literature review. Section 3 describes the method and defines the different transportation scenarios and driving cycles. In Section 4, the results of the simulations and optimizations are presented. Section 5 provides a detailed interpretation of the results, their sensitivity to some of the input parameters, and presents a related discussion. Finally, in Section 6, the conclusions of the study are presented. Furthermore, this section is followed by appendices, where the optimization problems are defined and the related data included.

2. Background

According to SAE standard (2016) J3016, a “driving automation system” (DAS) refers to any system or feature that performs the entire or part of a dynamic driving task. According to this standard, DAS is categorized into five levels. As part of a dynamic driving task, a level–1 DAS (i.e., driver assistance) controls either the lateral or longitudinal motion, and a level–2 DAS (i.e., partial driving automation) controls both lateral and longitudinal motions. For example, emergency braking involves level–1 DAS, whereas operational functions such as longitudinal vehicle motion control through acceleration and deceleration for following a reference speed

and changing lanes belong to level–2. A level–3 DAS (i.e., conditional driving automation) is capable of performing the entire dynamic driving task, but the driver should be ready to intervene upon system request. In levels 1–3 of a DAS, the presence of a human driver is essential in the cabin. In level–4 (i.e., high driving automation) or 5 (i.e., full driving automation), a DAS is capable of performing the entire dynamic driving task, including bringing the vehicle to a minimal risk condition in case of a failure. According to SAE standard (2016) J3016, ADS refer to levels 3–5, where the DAS can perform the entire driving, and a vehicle equipped with level–4 or level–5 DAS is referred to as an ADS–dedicated vehicle (ADS–DV). In levels 4 and 5, the presence of a human driver is not needed in the vehicle; instead, a remote dispatcher verifies the operational readiness of the vehicle and performs the dynamic driving task remotely, whenever necessary. High DAS and full DAS differ in their operational design domains. Operational design domain refers to the conditions under which a given DAS is designed to operate. A high DAS is limited to a specific operational design domain, whereas a full DAS is designed to function on all roads and conditions that are navigable by a human driver. The subject of this study was ADS–DVs, i.e., levels 4 and 5 of DAS.

TCO is usually used for comparative analysis of the competitive technologies, e.g., vehicles with different powertrains, and provides a good means of estimating profitability, according to, e.g., Davis and Figliozzi (2013), Feng and Figliozzi (2013), Lee et al. (2013), Taefi et al. (2015), Wu et al. (2015), Lebeau et al. (2015), Hagman et al. (2016), Taefi et al. (2016a), Taefi et al. (2017), Pelletier et al. (2016), Wadud (2017), Palmer et al. (2018), and Lebeau et al. (2019). TCO measures the life cycle cost, including the operational costs and the depreciation of the purchase price. Operational costs usually include the costs of fuel, maintenance, tax, insurance, and electric energy in the case of battery electric vehicles. In addition, in the case of commercial ADS–DVs, the operational costs associated to remote dispatchers are also included. Purchase price comprises vehicle hardware costs and, in the case of ADS–DVs, the cost of additional sensors and investment on remote dispatchers as well.

Wadud (2017) investigated the potential adoption of ADS–DVs on public roads by performing TCO analysis of private and commercial vehicles. The commercial vehicles included taxis and conventional trucks with gross mass of 7.5, 18 and 38 ton. They concluded that the commercial vehicles benefit more from automation, specially small trucks and taxis, because a large share of TCO belongs to the driver cost in small commercial vehicles. They, however, did not discuss electric vehicles.

The literature about TCO of road vehicle competitive powertrain technologies all involve human drivers. As such, Wu et al. (2015), Hagman et al. (2016) and Palmer et al. (2018) are concerned with passenger cars. Vehicle types, operations and purchase decisions are, however, different in road freight transport.

In road freight transport sector, Davis and Figliozzi (2013), used a cost function similar to TCO together with powertrain and logistics constraints. They compared the cost of two different battery electric and one conventional trucks on 243 transportation and driving scenarios with different costumer demands and operating speeds. The battery electric trucks had about 7.5 ton gross mass and 161 km driving range. The authors concluded that high utilization, low speed, frequent stops, tax incentives, and planning time horizon, i.e. vehicle life time, beyond 10 years can help the competitiveness of the electric trucks against conventional counterparts.

Feng and Figliozzi (2013) implemented a fleet replacement optimization framework that allowed replacing the conventional trucks with the battery electric trucks. They compared a small electric truck with a conventional truck of the same size on six different scenarios. The driving range of the electric truck was 161 km. They concluded that the electric truck can be cost effective if the annual utilization level is high.

Lee et al. (2013) compared TCO of a battery electric and a conventional truck with maximum gross mass of 7.49 ton on two driving cycles. The driving range of the electric truck was 161 km. They concluded that the relative benefits of electric trucks depend on vehicle efficiency associated with the driving cycle, diesel fuel price, battery price and replacement, charging infrastructure, and purchase price. They showed that the electric truck had lower TCO compared to the conventional one, without including subsidies, for a driving cycle with frequent stops and a low average speed.

Taefi et al. (2015) analyzed profitability concept of existing urban freight battery electric vehicles by interviewing companies to examine whether and how they operate profitably. Also, they performed a statistical analysis in Europe north sea region to capture the trends of the existing electric urban freight transport. The study identified two current trends of deploying electric vehicles in urban freight transport in north Europe: 1) slow and light electric vehicles, 2) medium heavy electric trucks in last mile logistics. In one of the cases, a concept truck of 12 ton gross mass was profitable that was achieved by considering measures in reduction of purchase and operational costs, and by increasing vehicle utilization. These measures included vehicle customization, subsidies and exemption from city toll, intermediate and quick charging, multi-shift operations, improvement of routing and scheduling, and etc.

Taefi et al. (2017) evaluated TCO considering battery health and replacement as a function of mileage at a given average energy consumption and warranted maximum mileage or maximum number of battery charge–recharge cycles. They calculated the cost-optimal mileage for three different electric trucks of about 12, 7.5 and 5 ton gross mass and ranges of 200, 160 and 120 km, respectively, and compared their TCO with the conventional counterparts. The authors used a fixed battery resale, i.e. rest, value regardless of the battery state of health as in the other literature. In their case, the electric trucks could not compete with conventional counterparts. They suggested that, in order to reduce TCO of each electric vehicle, the best cost-effective mileage should be calculated and planned, rather than selling the vehicle at a time when the battery end of life is reached.

Lebeau et al. (2015) and Lebeau et al. (2019) also evaluated TCO for several different light commercial vehicles. They concluded that these vehicles could compete with conventional counterparts if the vehicle utilization is high, and with the help of governmental subsidies. In addition, they showed that the period of ownership, the residual value and second life of the battery effect TCO of electric light commercial vehicles.

Reviewing the current available literature, the following gaps can be identified.

– TCO analysis of the battery electric ADS–DVs, e.g. ADS–DV BEHVs, is not conducted in the literature, and hence, no comparison is

made against the BEHVs with human drivers.
- Even though the literature suggests that vehicle customization based on the use case helps cost effectiveness of the battery electric trucks, the implications of such a customization on TCO is not studied in the literature. Consequently, there is no TCO minimization for varying vehicle parameters, e.g. battery size.
- The literature neglects energy consumption evaluation based on longitudinal vehicle dynamics on roads of different topographies and speeds. Thus, the cost–effectiveness of BEHVs is not investigated for different road hillinesses.
- TCO calculation of the electric vehicles in the literature does not include the driver cost, and thus neglects additional driver cost as a result of waiting time for charging during operation of the electric vehicles, compared to the conventional vehicles. Similarly, the trade-offs between the driver cost and charging time, battery degradation, charging power and cost, LU time and cost, and slow driving are neglected in TCO calculations.
- TCO analysis of battery electric trucks does not include trucks weighting more than 12 ton, and thus, possible transportation scenarios where BEHVs could be competitive to their conventional counterparts (with or without human drivers) are not identified.

This study tried to fill the above gapes and supports all the previous reports on the factors reducing TCO of the electric vehicles; in addition, we emphasized on the importance of the vehicle–infrastructure simultaneous optimization for a given transportation scenario. Optimizing vehicle–infrastructure is useful for the reason that TCO comparison of different BEHVs by itself does not reflect the profitability, owing to the performance constraint imposed by the range and power of batteries. Nevertheless, this problem can be overcome by sizing the batteries for a given transportation scenario. Moreover, the properties of a driving cycle such as road topography (i.e., hilliness), speed, and distance traveled influence vehicle performance, especially that of BEHVs. Thus, in this study, the performance and TCO of the optimum vehicle propulsion system were evaluated and compared for transportation tasks of different characteristics.

Furthermore, full automation of freight transport involves automation of LU to replace the role of the driver that performs part of this task. Automated guided vehicle systems (AGVS), developed with the purpose of optimizing material flow and reducing personnel, as reported by Flämig (2016), can be used for automated LU. AGVS facilitate 24/7 operation of vehicles, because they navigate automatically by themselves and perform well, owing to the repetitive nature of the operations. AGVS have been widely deployed in the industry and warehouses to reduce the TCO, especially in multishift operations, as reported by Ullrich (2015) and Liu et al. (2004). However, there exists no standard yet for automated truck loading and unloading. Furthermore, the utilization of charging stations at the LU point or consumer locations is motivated by the fact that it saves cost and time compared to the use of publicly scarce charging stations, according to Kopfer and Vornhusen (2017), and that virtually no high–power charging stations are available yet for BEHVs. Moreover, it will be more feasible if charging can be accomplished during the same time as performing LU, as reported by Taefi et al. (2016a) among measures of supporting freight electric vehicles. Thus, this study included the cost of infrastructure in the calculation of the TCO which comprises the cost of LU and charging stations.

3. Methodology

The influence of different aspects that are related to the transportation task and vehicle propulsion system was studied for ADS and vehicle electrification. More specifically, these aspects included the following.

- Transportation task
  - Vehicle size
  - Driving cycle, i.e., the distance between charging stations and LU points, average reference speed, and road hilliness
  - Infrastructure, i.e., charging power and LU scheme
- Vehicle propulsion system
  - Type of battery
  - Size of battery
  - Type of electric motors
  - Number of electric motors
  - Size of internal combustion engine (ICE)

The different aspects of the transportation task and vehicle propulsion system explained above were examined on four different plans. The plans concern different DAS levels and vehicle sources of power, shown in Table 1.

In this study, the operational design domain of the DAS comprised all defined transportation tasks, including all the trips, roads,

Table 1
Plans concerning the DAS levels and vehicle power source.

	CHV	BEHV
With driver (level–2 or level–3)	Plan–1	Plan–2
Without driver (level–4 or level–5)	Plan–3	Plan–4

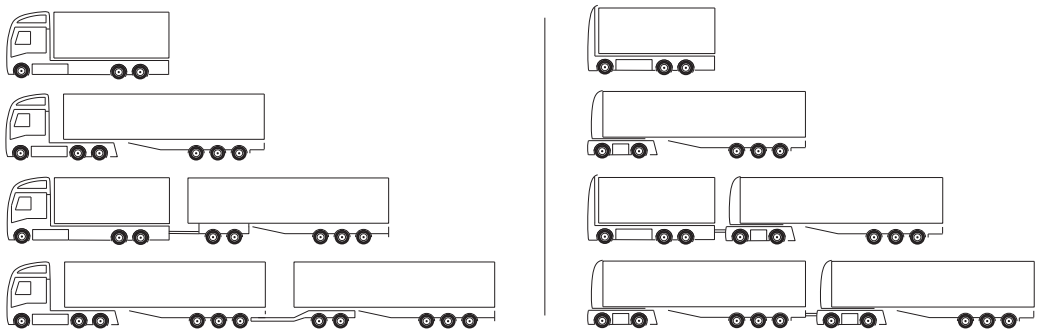

Fig. 1. Different sizes of freight heavy ADS–DV combinations (right) and heavy vehicle combinations with human drivers (left). Vehicles, from the smallest to the largest, are respectively called “rigid truck,” “tractor–semitrailer,” “Nordic combination,” and “A-double.”.

and dynamic driving tasks within them. Furthermore, vehicles were designed to operate exclusively on their assigned transportation tasks during their entire service life. Moreover, the ability of vehicles to operate outside the assigned transportation task might be constrained mainly by the propulsion system, and not by the DAS. Hence, in this study, the ability of vehicles to operate outside the operational design domain as governed by DAS was not emphasized, thereby including both levels 4 and 5 in a single plan.

In addition, it should be noted that, in all the plans, vehicles were equipped with a DAS higher than level–1, which meant that they all benefited equally from the eco–driving and fuel/energy efficiency offered by the DAS, as reported by Mersky and Samaras (2016) and Brown et al. (2014).

After the exclusion of the driver on–board in ADS–DVs, they can be considered to be without driver interfaces, such as steering, braking, and acceleration input devices. Moreover, given the purpose of exclusive freight transport, all seats and the cabin can be removed. Fig. 1 depicts the freight heavy ADS–DV combinations of different sizes, as well as the heavy vehicle combinations with human drivers, that were considered in this study. These vehicles are called “rigid truck,” “tractor and semitrailer,” “Nordic combination,” and “A-double” from the smallest to the largest, in that order.

3.1. Transportation task

A transportation task is defined by a distribution network comprising nodes, the routes between them, and pick-up/delivery demands. In this study, a distribution network included only two nodes. A vehicle was completely loaded/unloaded at each node while charging (in the case of BEHVs). Different transportation tasks were considered with driving cycles, i.e., different distances between nodes, road hillinesses, and average reference speeds, in order to investigate their influences on the incorporation of ADS and electrification. Average reference speed refers to the speed that a vehicle tries to maintain during the entire trip. Moreover, it was assumed that there always existed goods that needed to be transported within the network, therefore, both ADS–DVs and vehicles with human drivers operated 24 h every day (24/7) on a repetitive basis. The sensitivity of the results to lower utilization levels was also revealed.

3.1.1. Road hilliness

To investigate the influence of road hilliness on vehicle performance and propulsion system, roads with different hillinesses were considered in this study. According to the definition of global transport application (GTA) reported in the papers by Edlund and Fryk (2004) and Pettersson et al. (2018), road hilliness was categorized into four levels: flat, predominantly flat, hilly, and very hilly. In order to not be restricted to a specific geographical area, the roads in the different categories were modeled mathematically in this study, according to the works of Johannesson et al. (2016) and Pettersson et al. (2016).

Let $L_H = 1000$ m be the selected hill length, $L_s = 50$ m sample road distance, σ_y variance in road slope, y_k slope of the road in percentage, and k road grid index. Then, the road topographic profile can be generated using an auto-regressive model:

$$y_k = a y_{k-1} + e_k \tag{1}$$

where,

$$e_k = \mathcal{N}\left(0, \sigma_e^2\right), \qquad \sigma_e = \sqrt{(1-a^2)\sigma_y^2}, \qquad a = \sin\left(0.5 - 2\frac{L_s}{L_H}\right) \tag{2}$$

where, $\mathcal{N}$ denotes a normal distribution with standard deviation σ_e. Finally, elevation z_k is given by

$$z_k = z_{k-1} + L_s \frac{y_k}{100} \tag{3}$$

Parameter σ_y determines the level of hilliness according to GTA. σ_y values in the ranges (0,1.3], (1.3,2.3], (2.3,3.2], and larger than 3.2 correspond to flat, predominantly flat, hilly, and very hilly roads, respectively. Roads of different lengths and hillinesses were generated using the model mentioned above by choosing σ_y as 0.5, 1.5, 2.5, and 3.5 for the different levels of hillinesses. As an

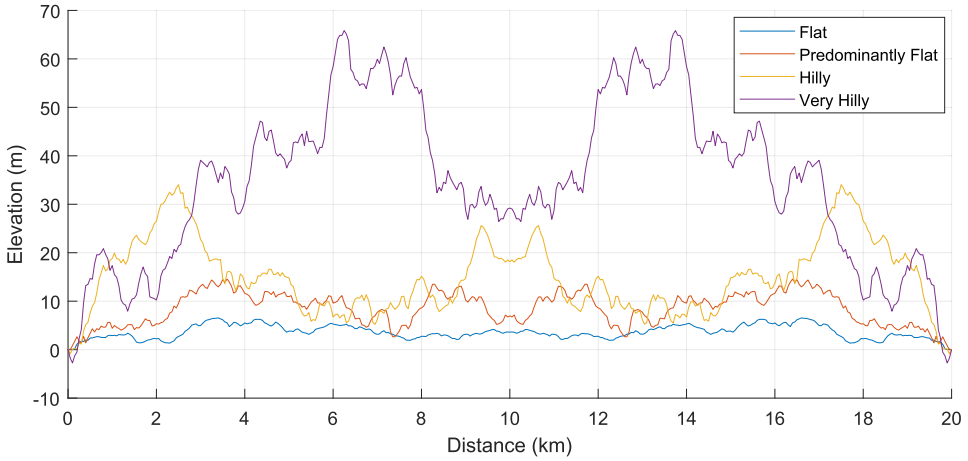

Fig. 2. Roads of length 10 km with different hillinesses. Elevation has been shown for back and forth travel between the two ends of the roads.

example, the different road elevations have been depicted in Fig. 2 for a road of length 10 km for travel back and forth between the two ends.

3.1.2. LU schemes

There is a trade–off between LU duration and TCO, because LU duration influences the temporal utilization level of a vehicle (i.e., vehicle-time on-road). Moreover, charging was considered to take place at the same time as LU occurred, thereby influencing the charging power required for providing sufficient energy to reach the next charging station. This study considered four LU schemes that were all executed automatically, mostly with the aid of AGVS, and are as follow.

- *on–board waiting*; in this case, vehicles wait until LU is performed by automated guided vehicles such as an automated lift-truck, which positions pallets of goods inside the containers using prescribed coordinates (Ullrich (2015)).
- *straddle carrier* (SC); in this case, containers can be lifted and carried by an automated straddle to assigned positions.
- *additional semitrailer* (AST); in this case, a semitrailer can be connected/disconnected to/from a tractor or dolly by an automated docking/undocking mechanism, while the vehicle is parked in a prescribed position.
- *on–board lift*; in this case, an on-board lift installed on the tractor and/or semitrailer is carried by the vehicle and automatically performs vehicle LU upon reaching the prescribed position.

The investment and operational cost of the LU schemes described above as well as their durations were considered in the evaluation of the TCO, and are provided in Appendix. It should be noted that the cost of emptying or filling an unloaded container was not considered, because it was not part of the transportation task and was constant in all the transportation scenarios.

3.2. Vehicle propulsion system

The most significant components of the propulsion system considered in this study include battery type and size, as well as electric motor type and number, in BEHVs; and the size of the ICE in CHVs. Given a source of power (i.e., battery or ICE), the role of human driver and ADS, vehicle size, and driving cycle, an optimum propulsion system was determined by minimizing the annual TCO per unit freight transported. The components of the propulsion system (i.e., the design variables) were selected from given discrete sets. The LU scheme and charging power at each node may also be considered as the design variables of the optimization problem. The optimization problems and constraints have been defined in Appendix.

3.3. Transportation mission management system (TMMS)

In real world, a driver may perform tasks other than dynamic driving; for example, assisting in LU or strategic functions such as trip scheduling and routing. These kinds of tasks are not performed by ADS. They are executed either automatically by AGVS or by a personnel/dispatcher as part of a TMMS. Dispatchers are responsible for monitoring the operational readiness of vehicles, as well as performing dynamic driving tasks remotely whenever necessary; for example, returning a vehicle to the depot in case of dynamic driving task performance–relevant system failure. A dispatcher may also perform strategic functions or monitor the functionality of AGVS for LU.

The costs pertaining to a TMMS include the operational costs such as the salary of the dispatcher and the equipment maintenance and investment cost related to, for example, a control tower. This study considered the following equivalent TMMS costs that resulted in the same annual cost.

– two personnel/dispatchers per fleet vehicle, each working 40 h per week with the same salary as that of a driver on a per hour basis;
– one personnel/dispatcher per fleet vehicle who works 40 h per week with the same salary as that of a driver on a per hour basis, and 350000 € on investment;
– one personnel/dispatcher for five fleet vehicles who works 40 h per week with the same salary as that of a driver on a per hour basis, and 620000 € on investment.

3.4. Cost function

The annual TCO per unit freight transported between two nodes C_t was considered as a measure of vehicle performance. The cost function includes the operational costs and the depreciation of the purchase price, and is defined as follows.

$$C_t = \frac{N_v(c_{elec} + c_{fuel} + c_{driver} + c_{maint} + c_{tax} + c_{insu} + c_{tmms}) + c_{dep}}{f_{tr}} \tag{4}$$

where N_v denotes the number of fleet vehicles; f_{tr} denotes the annual number of freight units transported in a round–trip between two nodes; c_{elec}, c_{fuel}, c_{driver}, c_{maint}, c_{tax}, c_{insu}, and c_{tmms} indicate the annual costs of electricity, diesel fuel, driver labor, vehicle maintenance, which includes tires, taxes, insurance, and TMMS, respectively; c_{dep} denotes the depreciation or yearly cost of investment and is defined as follows.

$$c_{dep} = \left(p - \frac{R_v}{(1+r)^{n_y}} + p_{batt,tot} - \frac{R_b}{(1+r)^{n_y}}\right)\frac{r}{1-(1+r)^{-n_y}} \tag{5}$$

where r, n_y, R_v, R_b, p, and $p_{batt,tot}$ denote the interest or discount rate, the economic life span in years, the vehicle–infrastructure resale value, the batteries resale value, and the purchase price of the vehicle–infrastructure excluding the batteries, and the purchase price of the all batteries including the replaced ones, respectively. The purchase price was calculated using the following equation and included the price of the vehicle chassis p_{chass}, cabin price, including driver interfaces p_{cab}, electric motors p_{em}, transmission systems p_{trans}, ICE p_{ice}, ADS p_{ads}, LU components p_{lu}, recharging infrastructure p_{rech}, and investment cost related to the TMMS such as that for a control tower.

$$p = N_v(p_{chass} + p_{cab} + p_{em} + p_{trans} + p_{ice} + p_{ads}) + p_{lu} + p_{rech} + p_{tmms} \tag{6}$$

Vehicle and battery-degradation models were implemented for calculating the operational and purchase costs in accordance with the works of Ghandriz et al. (2016) and Ghandriz et al. (2017). The maintenance cost of BEHVs was considered as 50% of that of CHVs, as suggested by Feng and Figliozzi (2013) and Lee et al. (2013). The ADS price p_{ads} includes the price of all the sensors and computers needed for object and event detection and response. Moreover, in BEHVs, the resale value of the vehicle–infrastructure might be different from that of last replaced battery depending on battery state of health. In this study, the batteries were replaced if the battery capacity reached 80% of the initial capacity, and their resale value was set to zero. A possible second life application, as reported by Lebeau et al. (2015), was neglected. In addition, for calculation of $p_{batt,tot}$, an yearly decrease in battery price, due to battery technology development, were considered. Furthermore, additional payload was allowed for BEHVs according to EU directive 2015/719, without considering any direct fiscal incentives. Please refer to Appendix A for further details.

By using such a cost function, optimization problems were defined to find an optimum vehicle–infrastructure design for a given scenario. A detailed definition of the optimization problems has been provided in Appendix A.

4. Results[1]

A scenario comprises a given road with its hilliness and distance between LU nodes or charging stations, and set average speed, vehicle size, powertrain type (i.e. battery electric or combustion–powered), and role of driver (i.e., ADS–DV or human driven). Combining all these parameters yields 3072 different transportation scenarios. For each of the scenarios and for a single vehicle in the fleet with 100% utilization, the vehicle–infrastructure optimization problem was solved and the results analyzed.

Fig. 3 reveals the annual TCO per unit freight as a function of the average reference speed of optimum tractor–semitrailers on a flat road with different lengths, as well as for different powertrains and roles of driver, when there is a single vehicle in the fleet and 100% utilization. Ghandriz et al. (2020) have provided the data and results for other vehicle sizes and road hillinesses. In the figure, each dot corresponds to an optimum vehicle–infrastructure and represents a solution of the optimization problem defined in Appendix A. It can be seen as to how the competitiveness of BEHVs against CHVs is affected by the distance between LU/charging nodes; moreover, reductions in TCO can be realized by using ADS in both BEHVs and CHVs. The following conclusions were drawn from Fig. 3.

– An optimized battery electric tractor–semitrailer with an optimized infrastructure can be more profitable than an optimized conventional combustion-powered tractor–semitrailer, if driving distances remain less than about 40 km for a vehicle with a

[1] A representative set of results has been provided in this paper. The complete set can be found in the paper by Ghandriz et al. (2020).

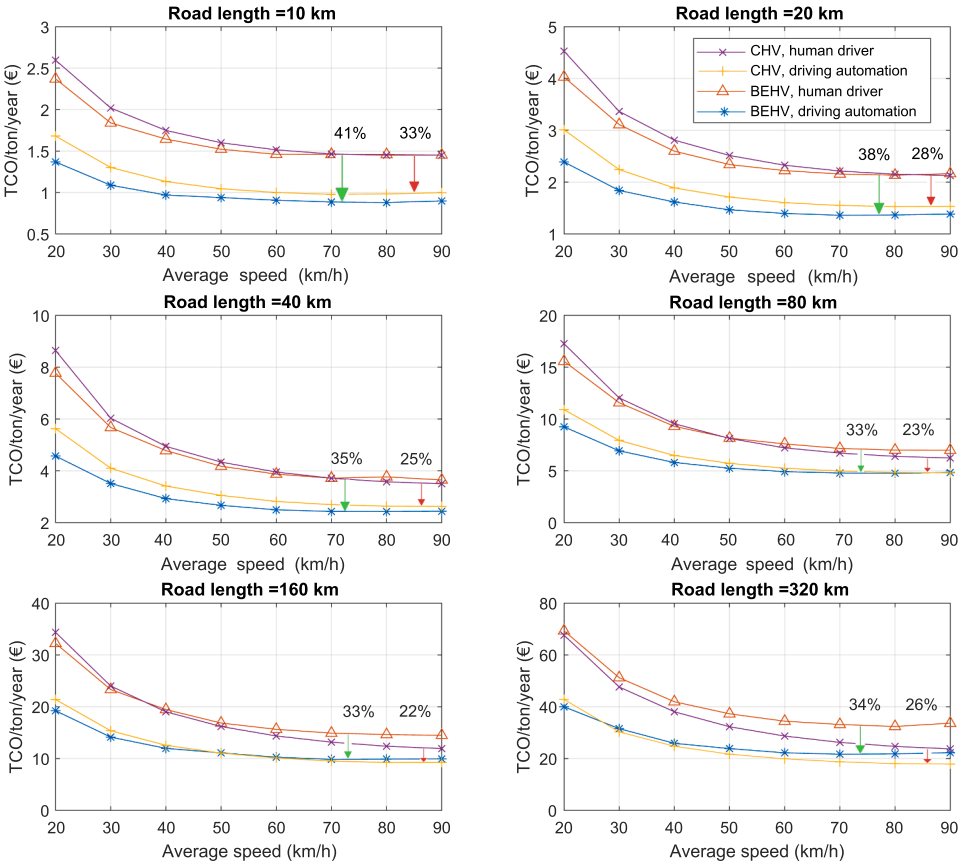

Fig. 3. Annual TCO per unit freight (ton) of optimum tractor–semitrailers for different plans. Each dot in the plots corresponds to an optimized vehicle–infrastructure on a flat road, when there is a single vehicle in the fleet. The reduction in cost achieved by driving automation is shown as percentages for BEHVs and CHVs. Vehicle utilization, i.e. vehicle time in operation, is 100% for all cases.

Table 2
Optimum vehicle–infrastructure of ADS–DV tractor–semitrailer and the one with human driver on a flat road of length 10 km.

	Reference speed	EM type	num. EM	BP type	num. BP	LU_1 [†]	LU_2	$P_{ch,1}$ [†] (kW)	$P_{ch,2}$ (kW)
ADS–DV	70 km/h	EM_2 [*]	4	BP_2^*	6	AST	AST	30	60
Human–driven vehicle	80 km/h	EM_2	4	BP_2	7	AST	AST	130	10

[*] Specifications of the electric motors (EMs) and battery packs (BPs), e.g., EM_2 and BP_2 are given in Appendix.
[†] LU_i: LU scheme at i^{th} node; $P_{ch,i}$: recharging power at i^{th} node.

human driver that is fully loaded on a flat road and with 100% utilization.

- The range of driving a profitable battery electric ADS-dedicated tractor–semitrailer increases to about 80 km, which is twice that of a vehicle with a human driver.
- The reduction in TCO achieved by electrification is higher in ADS–DV than in the vehicle with a human driver; likewise, the reduction in TCO achieved with ADS is higher in BEHVs than in CHVs.
- The optimum average driving speed is different for different powertrains and roles of driver. The optimum average reference speed is between 60 and 80 km/h for a battery electric ADS–DV, whereas it is between 70 and 90 km/h for a BEHV with a human driver. A higher optimum average reference speed is observed for CHVs.
- The TCO changes slightly within the range of average reference speeds between 50 and 90 km/h, in BEHVs, whereas the change in the TCO with speed is steep in CHVs, being up to 90 km/h.

It was also observed that the optimum vehicle–infrastructure (i.e., the type and number of electric motors, type and number of battery packs, LU schemes, and recharging power (P_{ch})) might be different in a battery electric ADS–DV and a battery electric vehicle with a human driver for driving at an optimum average reference speed on the same road. An example has been provided in Table 2. It must be noted that the optimum average reference speed might also be different in the two cases.

Furthermore, the effect of electrification and automation on different vehicle sizes was studied. The results for a scenario with a

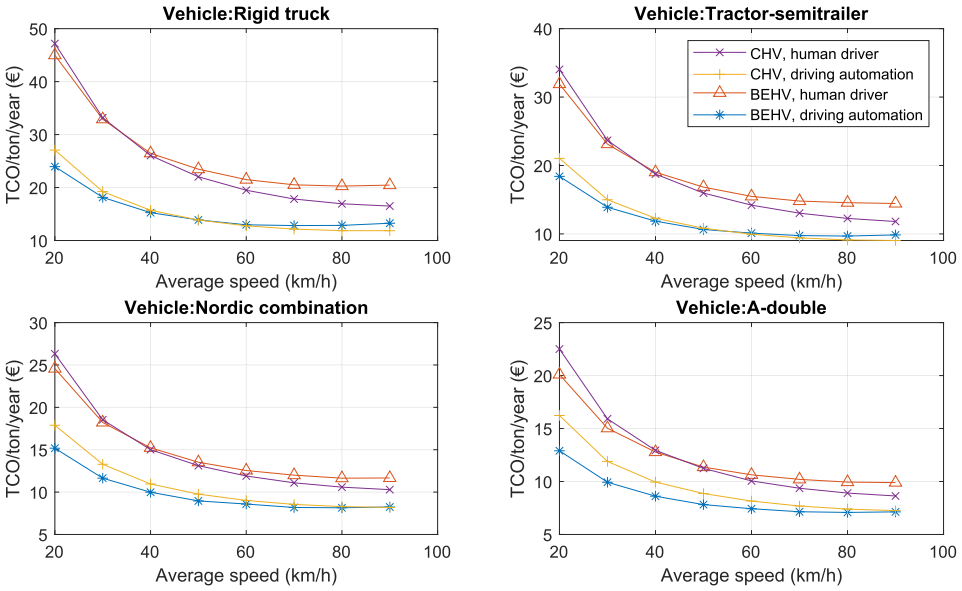

Fig. 4. Annual TCOs per unit freight (ton) of optimum vehicles with different sizes on a flat road of length 160 km. Each dot in the plots corresponds to an optimized vehicle–infrastructure. Vehicle utilization, i.e. vehicle time in operation, is 100% for all cases.

flat road of length 160 km are presented in Fig. 4. Please refer to the paper by Ghandriz et al. (2020) for the results for other roads. It can be seen that battery electric Nordic combination and A-double equipped with ADS display lower TCOs than those vehicles with human drivers up to the travel range of 160 km.

The hilliness of a road was also observed to affect the competitiveness of BEHVs. Fig. 5 reveals the annual TCO per unit freight for a tractor–semitrailer on a 160 km road with different hillinesses. The results for other vehicle sizes and road lengths are provided in the report by Ghandriz et al. (2020). It can be seen that the distance between the cost curves of a vehicle with a human driver increases with an increase in hilliness. Moreover, a battery electric ADS–DV almost affords a lower cost than a CHV on a 160 km flat road, whereas such a vehicle completely loses its competitiveness on a very hilly road of the same length. The reason is that hilly roads require large batteries. As an example, the optimum vehicle–infrastructures of tractor–semitrailers equipped with ADS have been shown in Table 3 for roads of length 160 km with different hillinesses.

The reduction in cost achieved with ADS–DV ranges between 27% and 46% for BEHVs and between 11% and 41% for CHVs for the different scenarios. Fig. 6 illustrates the cost components of vehicles with different sizes for different roles of driver (i.e., ADS–DV and a

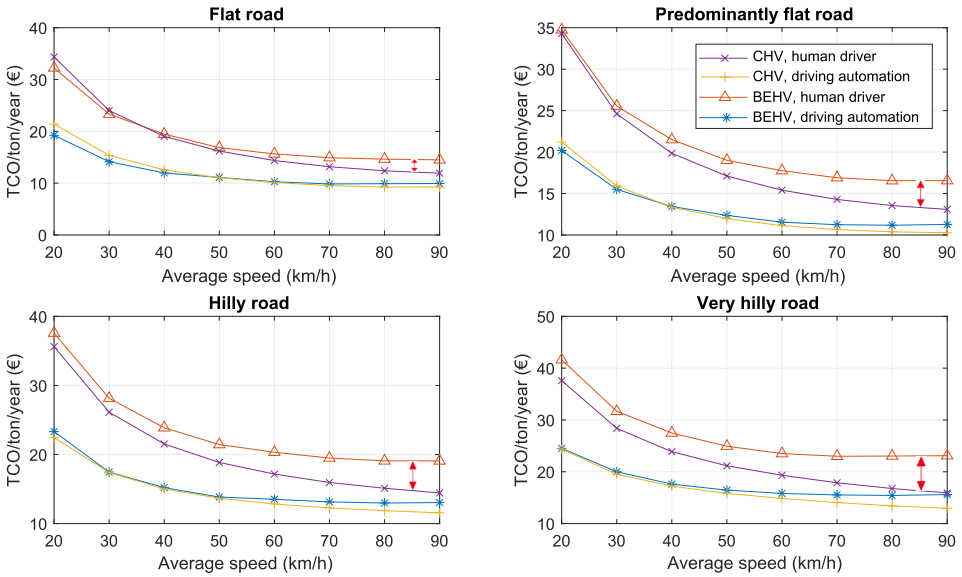

Fig. 5. Annual TCO per unit freight (ton) of an optimum tractor-semitrailer on a 160 km road with different hillinesses. Each dot in the plots corresponds to an optimized vehicle–infrastructure. Vehicle utilization, i.e. vehicle time in operation, is 100% for all cases.

Table 3
Optimum vehicle–infrastructure of ADS–dedicated tractor–semitrailer on a flat road of length 160 km.

Hilliness	Reference speed	EM type	num. EM	BP type	num. BP	LU_1 [†]	LU_2	$P_{ch,1}$ [†] (kW)	$P_{ch,2}$ (kW)
Flat	70 km/h	EM_1 [*]	4	BP_2 [*]	9	AST	AST	240	180
Predominantly flat	70 km/h	EM_1	4	BP_2	11	SC	SC	270	200
Hilly	70 km/h	EM_1	4	BP_2	13	SC	SC	300	250
Very hilly	70 km/h	EM_1	8	BP_2	15	SC	SC	300	270

[*] Specifications of EM and BP types are given in Appendix.
[†] LU_i: loading/unloading scheme at i^{th} node; $P_{ch,i}$: recharging power at i^{th} node.

Table 4
Optimum vehicle–infrastructures of different vehicles and plans on a flat road of length 160 km.

Powertrain, Driver role	Optimum reference speed	ICE[*] (lit)	EM type	num. EM	BP type	num. BP	LU_1 [†]	LU_2	$P_{ch,1}$ [†] (kW)	$P_{ch,2}$ (kW)
Rigid truck										
BEHV, HD	80 km/h	–	EM_2^*	2	BP_2^*	8	SC	SC	190	190
BEHV, ADS–DV	70 km/h	–	EM_2	2	BP_2	7	SC	SC	140	130
CHV, HD	90 km/h	6	–	–	–	–	SC	SC	–	–
CHV, ADS–DV	90 km/h	6	–	–	–	–	SC	SC	–	–
Tractor-semitrailer										
BEHV, HD	80 km/h	–	EM_1	4	BP_2	11	SC	SC	300	300
BEHV, ADS–DV	70 km/h	–	EM_1	4	BP_2	9	AST	AST	240	180
CHV, HD	90 km/h	8	–	–	–	–	AST	AST	–	–
CHV, ADS–DV	90 km/h	8	–	–	–	–	AST	AST	–	–
Nordic combination										
BEHV, HD	90 km/h	–	EM_1	6	BP_2	16	SC, SC	SC, SC	300	210
BEHV, ADS–DV	80 km/h	–	EM_3	4	BP_2	15	SC, SC	SC, SC	230	200
CHV, HD	90 km/h	11	–	–	–	–	SC, SC	SC, SC	–	–
CHV, ADS–DV	90 km/h	11	–	–	–	–	SC, SC	SC, SC	–	–
A-double										
BEHV, HD	90 km/h	–	EM_2	6	BP_2	21	SC, SC	SC, SC	30	30
BEHV, ADS–DV	90 km/h	–	EM_2	6	BP_2	19	SC, SC	SC, SC	300	300
CHV, HD	90 km/h	13	–	–	–	–	SC, SC	SC, SC	–	–
CHV, ADS–DV	90 km/h	13	–	–	–	–	SC, SC	SC, SC	–	–

[†] LU_i: LU scheme at i^{th} node for the first unit/semitrailer and second semitrailer (if any); $P_{ch,i}$: recharging power at i^{th} node.
[*] Specifications of ICE, EM and BP types are given in Appendix.

human-driven vehicle) and types of propulsion systems (i.e., battery electric and combustion–powered) on a flat road of length 160 km. It can be seen that the cost reduction achieved with ADS–DV is larger for BEHVs than CHVs in all the cases. Moreover, the cost reduction is lower for larger vehicles. The optimum vehicle–infrastructure designs corresponding to the scenarios shown in Fig. 6 can be found in Table 4.

5. Discussion

It has been demonstrated that the employment of ADS renders BEHVs competitive with CHVs over longer travel ranges compared to that of BEHVs with human drivers. Moreover, the optimum propulsion system setup and infrastructure of an ADS–dedicated BEHV was observed to be different from that of a BEHV with a human driver, in addition to differences in the vehicle hardware such as cabin, driver interfaces, sensors, computers, and actuators. ADS result in BEHVs with lower TCOs, mainly owing to there being no need to heat the cabin in ADS–DVs, as is the case when a human driver is involved, as well as the reduced optimum speed in ADS–DVs, which makes it possible to use smaller batteries. For a given transportation scenario, if a similar propulsion hardware as in a BEHV with a human driver is used in an ADS–dedicated BEHV, then the TCO might increase between 0% and 25%, compared with that of a ADS–dedicated BEHV with a uniquely designed propulsion system, depending on the vehicle size and transportation scenario. However, no change in the optimum propulsion hardware (i.e., the ICE) was observed in CHVs when replacing the human driver by ADS. Moreover, it was revealed that the TCO might increase by up to 35% if a BEHV designed to operate in a travel range of 80 km was instead used in transportation tasks where the travel ranges are only 10 km, regardless of whether it was a ADS–DV or not. It can be concluded that, in order to ensure competitiveness across different scenarios, the propulsion hardware should be adapted to the use case of BEHVs, irrespective of whether a human driver is involved. Such an adaptation, performed by vehicle–infrastructure optimization, explains why BEHVs with human drivers showed lower TCO than CHVs with human drivers, in many transportation scenarios of short road lengths, which was not observed in the literature before.

ADS reduce the TCO of BEHVs in all scenarios, but do not decrease it sufficiently to make them competitive with ADS–dedicated

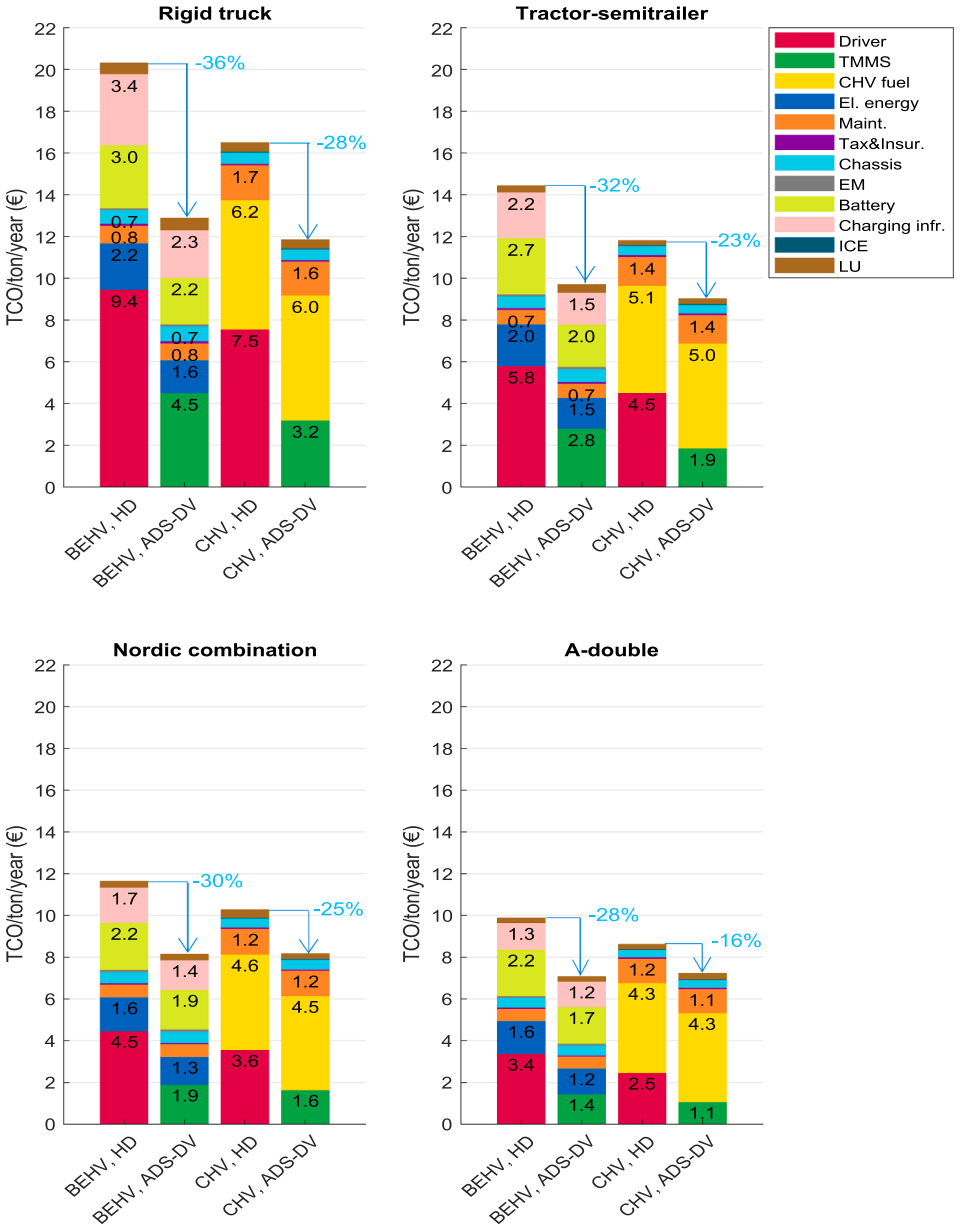

Fig. 6. Contributions of the different cost components to the annual TCO per unit freight (ton) of optimum vehicles with different sizes on a 160 km flat road. The cost structure has been shown for different optimum propulsion systems (BEHV and CHV) and infrastructure (LU and charging power), and for different roles of driver (i.e., ADS–DV and human–driven (HD)). The cost of ADS specific hardware is included in the chassis price.

CHVs on long and hilly roads. It has already been reported by Davis and Figliozzi (2013) that having many starts and stops in the driving cycle helps improve the competitiveness of BEHVs, owing to the possibility of energy recuperation. With this reasoning, it can be concluded that the hilliness of a road can exhibit a positive effect on the competitiveness of BEHVs owing to the recuperation of energy downhill. However, this reasoning is not entirely correct for BEHVs. In this study, it was observed that the hilliness of a road displays a negative effect on the competitiveness of BEHVs. On a hilly road with a grade of 11.5%, negotiation of the grade at the speed of 10 km/h requires approximately 2100% more power than what is needed for moving the vehicle on a flat road. Therefore, on hilly roads, the battery size is constrained by the power, and not by the energy needed for completing the trip, consequently, a larger battery is required. Moreover, frequent charging–discharging of batteries increases their degradation and shortens their service life. Consequently, the gain in cost due to energy recuperation is not comparable to the cost of the large battery, which renders BEHVs less competitive than CHVs on hilly roads. Contrary to this observation is the case when a power–optimized battery is used on short roads, or a vehicle is equipped with both power–optimized and energy–optimized batteries.

The optimum reference speed was observed to be lower in BEHVs than in CHVs, which is in accordance with the results reported

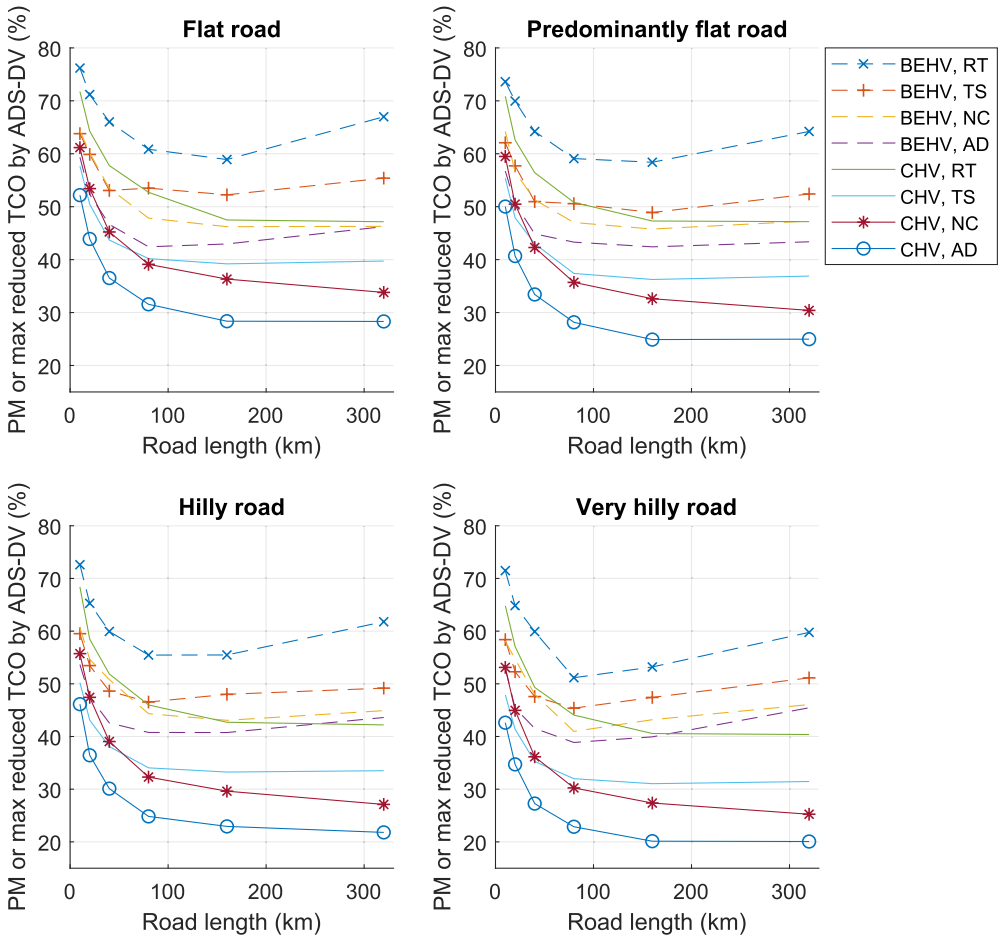

Fig. 7. Profit margin (PM) or the maximum reduced TCO achievable by employing ADS–DV, compared to a vehicle with a human driver, after considering a very low TMMS cost. The plots relate to different scenarios, and vehicle sizes: rigid truck (RT), tractor–semitrailer (TS), Nordic combination (NC), and A–double (AD).

by Taefi et al. (2016b), Lee et al. (2013). Likewise, ADS–dedicated BEHVs reveal lower optimum reference speeds than BEHVs with human drivers. The reason for this is difference in the energy consumption model and trade–offs between the power and battery size required in BEHVs and the absence of driver cost in ADS–DVs. However, the optimum reference speed seemed to converge to a high value (90 km/h) in large vehicles for all the scenarios as the depreciation cost increased; please refer to Table 4. Slow driving can be important for employing ADS–DVs on–road, because there are high safety requirements that need to be met along with technological limits on object and event detection and response. Thus, slow driving in ADS–dedicated BEHVs, with the corresponding optimum propulsion system setup, can yield the dual benefits of increased safety and reduced TCO, as in some transportation scenarios where the optimum speed of BEHVs is about 60 km/h. Moreover, the plots of annual TCO versus optimum reference speed reveal a mild slope for the TCO curve at a reference speed higher than 50 km/h in ADS–dedicated BEHVs. Therefore, if slow driving at 50 km/h is required, the resulting additional expense will be up to 10% of the TCO in BEHVs, whereas it can be up to 23% in CHVs.

It can be seen in Fig. 6 that the cost reduction achieved with ADS is lower for larger vehicles. The reason is that the contribution of driver cost to the annual TCO is lower for larger vehicles, whereas the costs of TMMS and ADS remain almost constant for all vehicle sizes. This observation is in accordance with the results of Wadud (2017).

The reduction in cost achieved with ADS is highly dependent on TMMS costs. TMMS cost comprises operational and investment costs. Operational cost refers to the expenditure associated with maintaining the ADS–related equipment and the salaries of dispatchers. Investment cost is related to equipment that include “control tower,” etc. The cost reduction achieved by employing ADS–DVs was observed to be between 27% and 46% for BEHVs and between 11% and 41% for CHVs for different scenarios, in the case of the assumptions regarding TMMS costs described in Section 3.3. Instead of analyzing the results for variations in the TMMS costs, the maximum achievable reduction in the TCO has been displayed in Fig. 7 for different scenarios, whereas both the operational and investment costs related to TMMS are considered to be very low owing to the inherent uncertainties in them. The results shown in Fig. 7 can be interpreted as the investment profit margin that is the maximum fraction of the cost of a vehicle with a human driver that can be invested/paid on a TMMS such that ADS–DV remains profitable compared to a vehicle with a human driver. The profit margin arises from the elimination of driver salary (35%–55%), an increased vehicle–time on–road owing to the fact that no

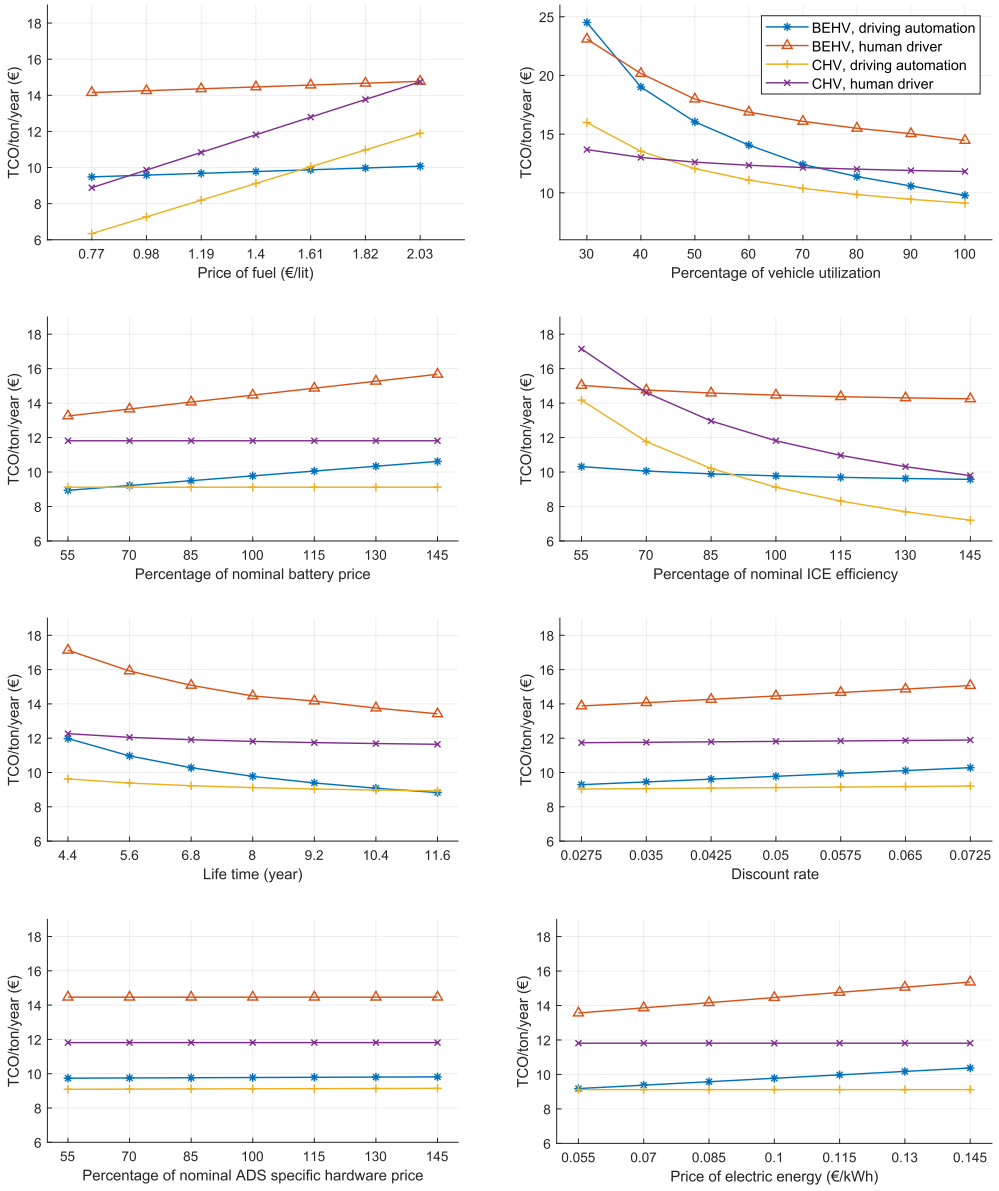

Fig. 8. Sensitivity of TCO to different parameters, namely, vehicle utilization level, fuel or ICE efficiency, life time, discount rate, and prices of diesel fuel, electric energy, battery, and ADS specific hardware, for a battery electric tractor–semitrailer on a 160 km flat road. Please refer to Appendix B for the. nominal values.

resting time is needed (0%–15%), an increased payload due to removal of the cabin (1.2%–5%), as well as from the optimized propulsion system (0%–20%), provided that both the vehicles are driven at a rate close to the optimum utilization rate as much as possible. It can be seen that the profit margin of ADS–dedicated BEHVs is larger than that of ADS–dedicated CHVs. Furthermore, larger vehicles reveal lower profit margins when employing ADS.

It must be noted that the results obtained may change if a different parametrization is used. The competitiveness of BEHVs is sensitive to the vehicle utilization level, fuel or ICE efficiency, life time, discount rate, and prices of diesel fuel, electric energy, battery, and ADS–specific hardware, i.e., on–board equipment for object and event detection and response. The nominal cost of equipment has been provided in Appendix, whereas the sensitivity of the TCO to these parameters, with lower and upper bounds of 45%, is given in Fig. 8 for a tractor–semitrailer on a 160 km flat road. For the same vehicle size and road, the components of the TCO for different vehicle utilization can be seen in Fig. 9. In these figures, vehicle utilization refers to the maximum fraction of the yearly time when the vehicle is in operation, i.e., when the vehicle is on–road or performs LU or charging; it includes the minimum rest time of the driver, as set by European Commission regulation 561/2006. It can be observed that for 30% utilization ADS–DVs are more expensive than vehicles with human drivers, mostly owing to high TMMS costs. It can also be seen that the price of ADS–specific hardware exhibits a minimal effect on the TCO, because it constitutes only a small fraction of the purchase and operational costs.

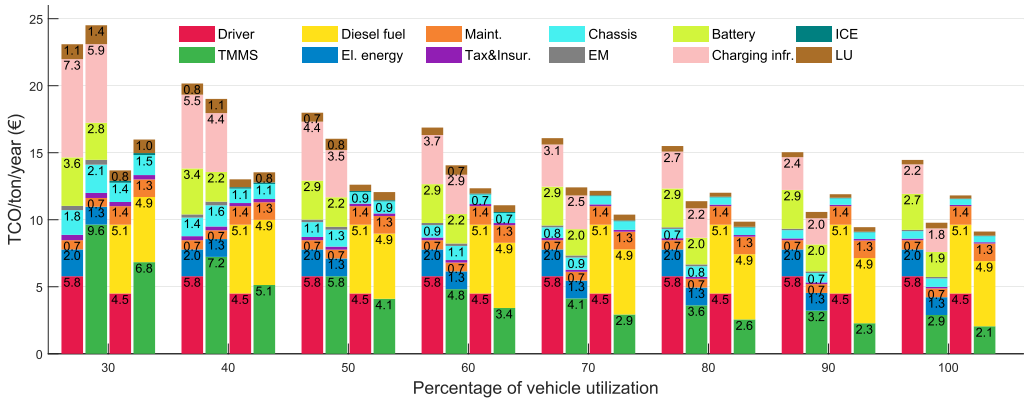

Fig. 9. Components of the TCO for different values of vehicle utilization for a battery electric tractor–semitrailer on a 160 km flat road. The cost of ADS–specific hardware is a part of chassis cost. In each group of four bars, similar to Fig. 6, from left to right, the bars represent BEHV HD, BEHV ADS–DV, CHV HD, and CHV ADS–DV.

Moreover, it should be noted that TCO of a BEHV also depends on the fuel consumption of a CHV, which operates in a same transportation task as the BEHV, as seen in the upper left plot in Fig. 8. The reason is that, based on the assumptions of this study, the maintenance cost of BEHVs is proportional to that of CHVs which is proportional to their fuel consumption. Please refer to the paper by Ghandriz et al. (2020) for the sensitivity results for other vehicles and roads, together with the changes in the cost components.

BEHVs can display a lower TCO if many vehicles can be employed in a fleet, whereby the cost per vehicle can be reduced by sharing the recharging station and LU infrastructure. In the case of employing 10 vehicles in a fleet, the ADS–dedicated battery electric tractor–semitrailer and the vehicle with a human driver can be competitive with their combustion–powered counterparts up to 320 and 160 km travel ranges, respectively, in case of 100% vehicle utilization, in contrast to a fleet comprising a single vehicle (shown in Fig. 3). Another scenario can involve excluding the cost of the charging infrastructure from the TCO, which will lead to more profitable BEHVs, as observed in Figs. 6 and 9, assuming that the size of the battery is not affected by the cost of the charging infrastructure. However, such a scenario cannot be considered to be realistic if no high–power charging stations are publicly available.

In the literature, e.g. Davis and Figliozzi (2013), Lee et al. (2013), Lebeau et al. (2015), Taefi et al. (2017), and Lebeau et al. (2019), usually, the large BEHVs with human drivers are not competitive to CHVs with human drivers. The main reasons are the high purchase cost of BEHVs, and that the driving range of the vehicles, studied in the literature, is usually about 160 km with 40%–60% vehicle utilization. The result presented in this study is in accordance with the literature. In this study, none of the BEHVs with human drivers, operating in a similar travel ranges and utilization as of the vehicles studied in the literature, are competitive to CHVs operating in the same conditions. However, in this study, BEHVs became competitive to CHVs in shorter travel ranges due to performing vehicle–infrastructure optimization, despite considering the cost of the charging infrastructure in TCO of BEHVs. Moreover, as larger the vehicle, the lesser is the difference between the annual TCO per unit freight transported of BEHVs and that of CHVs with human drivers, as can be seen in Figs. 4 and 6. The main reason is that charging infrastructure depreciation cost per unit freight transported reduces considerably in the case of a large BEHV, similar to the case when several small BEHVs are used in a fleet.

Finally, the performance of BEHVs can be further improved by considering additional incentives or the higher taxes imposed on CHVs through regulations. Furthermore, electric road systems and dynamic charging, whereby charging is possible on–road while driving, entirely facilitate the competitiveness of BEHVs, as reported by Alaküla and Márquez-Fernández (2017) and Fyhr et al. (2017). Moreover, further reductions in fuel and energy consumption can be achieved by implementing speed profile optimization on–road considering the topography, and within the maximum and minimum speed limits around the reference speed according to, for example, the works of Johannesson et al. (2015), Hovgard et al. (2018), and Torabi and Wahde (2018). A requirement for maintaining the set optimal speed is that the motion of the vehicle is not abstracted much by the surrounding traffic, such as driving in a dedicated lane, or by an “intelligent traffic management system” that controls the entire traffic, as reported by Milanes et al. (2012).

6. Conclusion

By implementing mathematical models together with optimum choices of vehicle–infrastructure through TCO minimization, this study identified those transportation scenarios, with or without human drivers, where utilizing BEHVs is more competitive compared to CHVs. Moreover, the study showed that ADS affect other vehicular systems, in particular, the optimum setup of the propulsion system of BEHVs. ADS lead to decreased TCO of between 27% and 46% for BEHVs and between 11% and 41% for CHVs, which render BEHVs profitable over longer travel ranges by a factor of four, compared to that of BEHVs with human drivers. Furthermore, the profitability of ADS–DVs as well as the competitiveness of BEHVs against CHVs has been demonstrated for different transportation scenarios. It was observed that ADS–dedicated BEHVs tend to exhibit lower optimal speeds than vehicles with human drivers. Moreover, the reduction in speed for safety reasons was shown to be less expensive to realize in ADS–dedicated BEHVs than in

ADS–dedicated CHVs; in many scenarios, low speeds down to 60 km/h actually reduced the TCO.

Furthermore, owing to the uncertainty in the parametrization, sensitivity tests were carried out. Moreover, the maximum reduction in the TCO that can be achieved by adopting ADS at a very low cost of TMMS was presented for different vehicles and roads. The reduction in the TCO in ADS–DVs was mainly achieved by removing the driver salary (35%–55%), increasing the vehicle–time on–road (0%–15%), increasing the payload by removing the cabin (1.2%–5%), as well as by optimizing the propulsion system (0%–20%).

Consideration of many transportation scenarios with different road types and vehicle sizes resulted in the production of a large volume of data. The data revealed that in order to achieve profitable operation with zero emission, the propulsion hardware should be adapted to the use case of BEHVs, irrespective of whether a human driver is involved. All the produced data and figures have been provided in Ghandriz et al. (2020) giving practitioners valuable information on the feasibility and profitability of an intended freight transport operation involving automation and electrification for a given use case.

However, the results of this study are limited to the repetitiveness of transport operations on known roads. Even though sensitivity analysis of the vehicle utilization can provide a rough estimate of the TCO for non–repetitive assignments, the optimum propulsion hardware cannot be reused, unless it is designed for the worst–case scenario where the vehicle is intended to operate, which requires more study. Furthermore, this study simplified a transportation scenario to include only one vehicle type and two pickup and delivery nodes. Future studies shall involve hardware–infrastructure optimization of a fleet of vehicles of different types that are operating in a transportation network comprising more number of nodes, where the optimum propulsion hardware for each vehicle and optimum location of charging stations will be determined based on minimization of the TCO.

CRediT authorship contribution statement

Toheed Ghandriz: Conceptualization, Methodology, Software, Validation, Formal analysis, Investigation, Data curation, Writing - original draft, Writing - review & editing, Visualization. **Bengt Jacobson:** Resources, Writing - review & editing, Supervision, Project administration, Funding acquisition. **Leo Laine:** Writing - review & editing, Supervision, Funding acquisition. **Jonas Hellgren:** Data curation, Writing - review & editing, Supervision.

Acknowledgment

This work was supported by the Swedish national research program FFI managed by Swedish Energy Agency.

Appendix A. Optimization problems

The optimum vehicle–infrastructure can be found by minimizing the annual TCO per unit freight transported $\widetilde{c}_t$ for a road with given length and hilliness, average vehicle reference speed, vehicle size, and plan that defines the driver role. Variable names with (~) on the top denote functions of other variables and input parameters, whereas all other variables denote either the given trajectories or input parameters that depend only on the design variables. The input parameters can be found in Tables B.6,B.7,B.8,B.9,B.10,B.11,B.12. The argument x, representing vehicle position along the road, together with other function arguments have been omitted from the equations for clarity of notations.

A.1. Conventional combustion–powered vehicles

The optimization problem was defined as follows for a CHV.

$$\begin{aligned}
&\text{find} && a_k \in \boldsymbol{S}_{CV,k} \in \boldsymbol{S}_{CV}, \quad k = 1,...,n_{sc} \\
& && \boldsymbol{S}_{CV} = \{\boldsymbol{S}_{CV,1},...,\boldsymbol{S}_{CV,n_{sc}}\} = \{\boldsymbol{type}_{ice}, \boldsymbol{LU}_{1stTr,1}, \boldsymbol{LU}_{2ndTr,2}, \boldsymbol{LU}_{1stTr,1}, \boldsymbol{LU}_{2ndTr,2}\} \\
&\text{to minimize} && \widetilde{C}_t = \frac{N_v(\widetilde{c}_{fuel} + \widetilde{c}_{driver} + \widetilde{c}_{maint,cv} + c_{tax} + c_{insu} + c_{tmms}) + \widetilde{c}_{dep}}{\widetilde{f}_{tr}} && \text{(A.1)} \\
&\text{subject to} && \widetilde{c}_{fuel} = p_f \widetilde{F}_c \widetilde{N}_t && \text{(A.2)} \\
& && \widetilde{c}_{driver} = p_d \widetilde{t}_{tr} \widetilde{N}_t && \text{(A.3)} \\
& && \widetilde{c}_{maint,cv} = c_m \widetilde{c}_{fuel} && \text{(A.4)} \\
& && \widetilde{f}_{tr} = \widetilde{N}_t N_v (m_{gcm} - (m_{chass} + m_{cab} + m_{ice} + m_{obl})) && \text{(A.5)} \\
& && \widetilde{c}_{dep} = \left(\widetilde{p} - \frac{\widetilde{R}_v}{(1+r)^{n_y}}\right) \frac{r}{1-(1+r)^{-n_y}} && \text{(A.6)} \\
& && \widetilde{p} = N_v(p_{chass} + p_{cab} + p_{trans} + p_{ice} + p_{ads}) + p_{lu} + p_{tmms} && \text{(A.7)} \\
& && \widetilde{R}_v = 0.15\widetilde{p} && \text{(A.8)}
\end{aligned}$$

$$\widetilde{N}_t = \frac{u\, T_{year}}{\widetilde{t}_{tr}} \tag{A.9}$$

$$\widetilde{F}_c = \frac{1}{E_{pgf}\, \eta_{ice}\, D_f} \int_0^{t_{tor}} \widetilde{P}_{ice}(t)\, dt \tag{A.10}$$

$$\widetilde{t}_{tor} = \int_0^{x_f} \frac{dx}{\widetilde{v}} \tag{A.11}$$

$$\widetilde{t}_{tr} = \widetilde{t}_{tor} + \sum_{i=1}^{2} \max\left(t_{lu,i},\ \widetilde{t}_{res,i}\right) \tag{A.12}$$

$$\widetilde{t}_{res,i} = \frac{45}{240}\frac{\widetilde{t}_{tor}}{2}, \quad i \in \left\{1, 2\right\} \tag{A.13}$$

$$\widetilde{P}_{ice} = \frac{1}{\eta_{ctr}} \widetilde{F}_{prop}\, \widetilde{v} \tag{A.14}$$

$$P_{ICE,min} \leqslant \widetilde{P}_{ice} \leqslant P_{ICE,max} \tag{A.15}$$

$$\widetilde{F}_{prop} = \widetilde{F}_{long} - \widetilde{F}_{fri} \tag{A.16}$$

$$\widetilde{F}_{long} = m_{gcm}\, \dot{\widetilde{v}} + \widetilde{F}_r \tag{A.17}$$

$$\widetilde{F}_r = m_{gcm}\, g\, f_r \cos(\phi) + \frac{1}{2}\rho_a\, A_f\, c_d\, \widetilde{v}^2 - m_{gcm}\, g \sin(\phi) \tag{A.18}$$

$$\dot{\widetilde{v}} = \begin{cases} \dot{v}_{ref}, & \widetilde{F}_{long,min} \leqslant \widetilde{F}_{long} \leqslant \widetilde{F}_{long,max} \\ \frac{\widetilde{F}_{long,max} - \widetilde{F}_r}{m_{gcm}}, & \widetilde{F}_{long} > \widetilde{F}_{long,max} \\ \frac{\widetilde{F}_{long,min} - \widetilde{F}_r + \widetilde{F}_{fri}}{m_{gcm}}, & \widetilde{F}_{long} < \widetilde{F}_{long,min} \end{cases} \tag{A.19}$$

$$\widetilde{F}_{long,max} = \min\left(\frac{\widetilde{T}_{max}\, Ratio_{max}}{R}, \frac{\widetilde{P}_{max}}{\widetilde{v}}\right) \tag{A.20}$$

$$\widetilde{F}_{long,min} = \max\left(\frac{\widetilde{T}_{min}\ Ratio_{max}}{R}, \frac{\widetilde{P}_{min}}{\widetilde{v}}\right) \tag{A.21}$$

$$\widetilde{P}_{max} = \eta_{ctr}\, P_{ICE,max} \tag{A.22}$$

$$\widetilde{P}_{min} = 0 \tag{A.23}$$

$$\widetilde{T}_{max} = \eta_{ctr}\, T_{ICE,max} \tag{A.24}$$

$$\widetilde{T}_{min} = 0 \tag{A.25}$$

$$\widetilde{F}_{fri} = \begin{cases} m_{gcm}\, \dot{v}_{ref} + \widetilde{F}_r, & \widetilde{F}_{long} < 0 \\ 0, & \text{otherwise} \end{cases} \tag{A.26}$$

$$\widetilde{G}_{CV} \geqslant G_{min} \tag{A.27}$$

$$\widetilde{S}_{CV} \geqslant S_{min} \tag{A.28}$$

$$\widetilde{A}_{CV} \leqslant A_{max} \tag{A.29}$$

where, a_k, $k = 1...n_{sc}$ denote the design variables of n_{sc} dimensional space $\boldsymbol{S}_{CV}$, in which the range of k^{th} dimension is specified by set $\boldsymbol{S}_{CV,k}$ containing discrete choices of the design variable a_k. The design variables of a CHV include the type of ICE, LU of the first unit/semitrailer at the first node of the transportation task, LU of the second semitrailer (if any) at the first node of the transportation task, LU of the first unit/semitrailer at the second node, LU of the second semitrailer (if any) at the second node, the ranges of which are denoted by $\boldsymbol{type}_{ice}$, $\boldsymbol{LU}_{1stTr,1}$, $\boldsymbol{LU}_{2ndTr,2}$, $\boldsymbol{LU}_{1stTr,1}$, and $\boldsymbol{LU}_{2ndTr,2}$, respectively, as presented in Table B.5. Different types of ICE are described in Table B.8 and different LU schemes are explained in Section 3.1.2. In the cost function (A.1), N_v denotes the number of vehicles, $\widetilde{f}_{tr}$ denotes the transported freight per year (described by Eq. (A.5)), and $\widetilde{c}_{fuel}$, $\widetilde{c}_{driver}$, $\widetilde{c}_{maint,cv}$, and $\widetilde{c}_{dep}$ denote the annual diesel cost, driver salary, cost of maintenance, and hardware depreciation, respectively, and are given by Eqs. (A.2), (A.3), (A.4) and (A.6),

respectively; c_{tax}, c_{insu}, and c_{tmms} denote the annual cost of taxes, insurance and TMMS, respectively. In Eq. (A.2), p_f, $\widetilde{F}_c$ and $\widetilde{N}_t$ denote the prices of diesel fuel, and the fuel consumed during a round–trip (described by Eq. (A.10)), and the number of trips a vehicle performs per year, respectively. In Eq. (A.3), p_d and $\widetilde{t}_{tr}$ denote driver salary and round–trip time, which are described by Eq. (A.12). Eq. (A.4) describes the maintenance cost proportional to the fuel cost that is quantified by a proportionality factor c_m. In Eq. (A.5), m_{gcm}, m_{chass}, m_{cab}, m_{ice}, and m_{obl} represent the masses of a fully loaded vehicle (i.e., gross combination mass), vehicle chassis, cabin, ICE, and on–board lift, respectively. Eq. (A.6) gives the depreciation cost of hardware based on interest rate r, service life span n_y, vehicle–infrastructure resale value $\widetilde{R}_v$ (described by Eq. (A.8)), and price of the vehicle–infrastructure $\widetilde{p}$, described by Eq. (A.7),including the chassis price p_{chass}, price of cabin along with driver interfaces p_{cab}, transmission price p_{trans}, ICE price p_{ice}, price of all the vehicle hardware required for ADS p_{ads}, investment cost of LU p_{lu}, and investment cost related to TMMS p_{tmms}. Eq. (A.9) gives the number of trips per year, where T_{year} stands for a time span of one year in the same unit as $\widetilde{t}_{tr}$, and $0 < u < 1$ represents vehicle utilization. It should be noted that the performance of a vehicle was simulated for an entire year.

The fuel consumed during a round–trip can be calculating using Eq. (A.10), where η_{ice}, E_{pgf}, D_f, t_{tor} and $\widetilde{P}_{ice}$ denote the maximum efficiency of ICE, energy per gram of diesel fuel, fuel density, travel time on road (described by Eq. (A.11)), and ICE power (described by Eq. (A.14)), respectively. In Eq. (A.11), x_f denotes the overall distance covered in the round–trip and $\widetilde{v}$ is the vehicle speed at the distance x on road, described by differential Eq. (A.19), where $(\dot{})$ denotes time derivative. In Eq. (A.12), $t_{lu,i}$ denotes the LU time and $\widetilde{t}_{res,i}$ represents driver resting time. A driver must rest 45 min after every four hours of driving, according to European Commission Regulation 561/2006 (Eq. (A.13)), when considering a transportation task involving two nodes. It must be noted that a driver can rest during LU process. In Eq. (A.14), η_{ctr} denotes transmission efficiency and $\widetilde{F}_{prop}$ denotes the total propulsion force on the vehicle tires, as described by Eq. (A.16). The ICE power is constrained between the minimum and maximum values, $P_{ICE,min}$ and $P_{ICE,max}$, according to constraint (A.15). Eq. (A.16) yields the propulsion force originating from the ICE, where $\widetilde{F}_{fri}$ denotes the friction brake force and $\widetilde{F}_{long}$ denotes the total longitudinal force, including the propulsion and friction brake. Eq. (A.17) describes Newtonian law of motion, wherein $\widetilde{F}_r$ is the resistance force described by Eq. (A.18). The resistance force (A.18) includes the rolling resistance of tiers, air resistance, and resistance force caused by gravity, wherein, g, f_r, ϕ, ρ_a, A_f, and c_d represent the gravitational constant, rolling resistance coefficient, grade of the road at distance x, air density, front area of the vehicle, and aerodynamic drag coefficient, respectively. In Eq. (A.19), v_{ref}, $\widetilde{F}_{long,min}$, and $\widetilde{F}_{long,max}$ denote the reference speed along the road, minimum available longitudinal force (described by Eq. (A.21)), and maximum available longitudinal force (described by Eq. (A.20)), respectively. In these equations, $Ratio_{max}$, R, $\widetilde{P}_{max}$, $\widetilde{P}_{min}$, $\widetilde{T}_{max}$, and $\widetilde{T}_{min}$ denote the maximum transmission gear ratio, radius of the wheels, maximum and minimum powers acting on the wheels (described by Eqs. (A.22) and (A.23)), and maximum and minimum torques acting on the wheels (described by Eqs. (A.24)), respectively. Furthermore, in Eqs. (A.22)–(A.25), η_{ctr}, $P_{ICE,max}$, $P_{ICE,min}$, $T_{ICE,max}$, and $T_{ICE,min}$ stand for the transmission efficiency and the maximum and minimum ICE output powers and torques. Eq. (A.26) gives the friction brake force required to reach the reference speed during negative acceleration. It should be noted that, in these equations, the grip limit between the road and the contact patch of the wheel is not considered.

Finally, the constraints (A.27)–(A.29) ensure proper vehicle performance on–road. Constraint (A.27) requires a gradeability higher than a set value. Gradeability is the maximum grade on which a vehicle is capable of maintaining a set forward speed (e.g., 80 km/h). Constraint (A.28) ensures that a vehicle is capable of starting the forward motion on a given grade, which is referred to as startability. Constraint (A.29) guarantees that the acceleration capability of a vehicle is higher than a minimum set value. These constraints were evaluated by programming based on their definitions. Edgar et al. (2002), Sadeghi Kati (2013), Sadeghi Kati et al. (2014), Kharrazi et al. (2015)) provide further descriptions of the performance–based characteristics of heavy vehicles.

A.2. Battery electric vehicles

Similar to the case of a CHV, the optimization problem for a BEHV was defined as follows.

$$\begin{aligned}
&\text{find} && a_k \in \boldsymbol{S}_{EV,k} \in \boldsymbol{S}_{EV}, \quad k = 1, \ldots, n_{se} \\
&&& \boldsymbol{S}_{EV} = \{\boldsymbol{S}_{EV,1}, \ldots, \boldsymbol{S}_{EV,n_{se}}\} = \{\boldsymbol{type}_{em}, \boldsymbol{N}_{em}, \boldsymbol{type}_{pack}, \boldsymbol{N}_{pack}, \boldsymbol{LU}_{1stTr,1}, \boldsymbol{LU}_{2ndTr,1}, \\
&&& \boldsymbol{LU}_{1stTr,2}, \boldsymbol{LU}_{2ndTr,2}, \boldsymbol{P}_{ch,1}, \boldsymbol{P}_{ch,2}\} \\
&\text{to minimize} && \widetilde{C}_t = \frac{N_v(\widetilde{c}_{elec} + \widetilde{c}_{driver} + \widetilde{c}_{maint,ev} + c_{tax} + c_{insu} + c_{tmms}) + \widetilde{c}_{dep}}{f_{tr}} \qquad \text{(A.30)}
\end{aligned}$$

$$\text{subject to} \quad \widetilde{c}_{elec} = p_{el}\,\widetilde{E}_{el}\,\widetilde{N}_t \qquad \text{(A.31)}$$

$$\widetilde{c}_{driver} = p_d\,\widetilde{t}_{tr}\,\widetilde{N}_t \qquad \text{(A.32)}$$

$$\widetilde{c}_{maint,ev} = 0.5\,\widetilde{c}_{maint,cv} \qquad \text{(A.33)}$$

$$\widetilde{f}_{tr} = \widetilde{N}_t N_v (m_{gcm} + m_{add} - (m_{chass} + m_{cab} + N_{em}\,m_{ElDrive} + N_{pack}\,m_{pack} + m_{obl})) \qquad \text{(A.34)}$$

$$\widetilde{c}_{dep} = \left(\widetilde{p} - \frac{\widetilde{R}_v}{(1+r)^{n_y}} + \widetilde{p}_{batt,tot} - \frac{\widetilde{R}_b}{(1+r)^{n_y}}\right)\frac{r}{1-(1+r)^{-n_y}} \qquad \text{(A.35)}$$

$$\widetilde{p} = N_v(p_{chass} + p_{cab} + p_{em} + p_{trans} + p_{ads}) + p_{lu} + p_{rech} + p_{tmms} \qquad \text{(A.36)}$$

$$\widetilde{R}_v = 0.15\widetilde{p} \tag{A.37}$$

$$\widetilde{p}_{batt,tot} = N_v \sum_{j=1}^{\widetilde{n}_{rep}} p_{batt}\,(1 - d_{bp})^{j\,\widetilde{n}_{yrep}} \tag{A.38}$$

$$\widetilde{N}_t = \frac{u\,T_{year}}{\widetilde{t}_{tr}} \tag{A.39}$$

$$\widetilde{E}_{el} = \int_0^{\widetilde{t}_{tor}} \widetilde{P}_{batt}(t)\,dt \tag{A.40}$$

$$\widetilde{t}_{tor} = \int_0^{x_f} \frac{dx}{\widetilde{v}} \tag{A.41}$$

$$\widetilde{P}_{batt} = \widetilde{P}_{em} + \widetilde{P}_{em,loss} + \widetilde{P}_{batt,loss} \tag{A.42}$$

$$P_{batt,min} \leqslant \widetilde{P}_{batt} \leqslant P_{batt,max} \tag{A.43}$$

$$\widetilde{P}_{em} = \begin{cases} \min\left(\frac{1}{\eta_{tr}}\widetilde{F}_{prop}\,\widetilde{v},\ P_{em,max}\right), & 0 \leqslant \widetilde{P}_{em} \\ \max(\eta_{tr}\,\widetilde{F}_{prop}\,\widetilde{v},\ P_{em,min}), & \widetilde{P}_{em} < 0 \end{cases} \tag{A.44}$$

$$\widetilde{F}_{prop} = \widetilde{F}_{long} - \widetilde{F}_{fri} \tag{A.45}$$

$$\widetilde{F}_{long} = m_{gcm}\,\dot{\widetilde{v}} + \widetilde{F}_r \tag{A.46}$$

$$\widetilde{F}_r = m_{gcm}\,g\,f_r\cos(\phi) + \frac{1}{2}\rho_a A_f\,c_d\,\widetilde{v}^2 - m_{gcm}\,g\sin(\phi) \tag{A.47}$$

$$\dot{\widetilde{v}} = \begin{cases} \dot{v}_{ref}, & \widetilde{F}_{long,min} \leqslant \widetilde{F}_{long} \leqslant \widetilde{F}_{long,max} \\ \frac{\widetilde{F}_{long,max} - \widetilde{F}_r}{m_{gcm}}, & \widetilde{F}_{long} > \widetilde{F}_{long,max} \\ \frac{\widetilde{F}_{long,min} - \widetilde{F}_r + \widetilde{F}_{fri}}{m_{gcm}}, & \widetilde{F}_{long} < \widetilde{F}_{long,min} \end{cases} \tag{A.48}$$

$$\widetilde{F}_{long,max} = \min\left(\frac{\widetilde{T}_{max}\,Ratio_{max}}{R},\ \frac{\widetilde{P}_{max}}{\widetilde{v}}\right) \tag{A.49}$$

$$\widetilde{F}_{long,min} = \max\left(\frac{\widetilde{T}_{min}\ Ratio_{max}}{R},\ \frac{\widetilde{P}_{min}}{\widetilde{v}}\right) \tag{A.50}$$

$$\widetilde{P}_{max} = \eta_{tr}\min(P_{batt,max} - \widetilde{P}_{em,loss} - \widetilde{P}_{batt,loss},\ P_{em,max}) \tag{A.51}$$

$$\widetilde{P}_{min} = \frac{1}{\eta_{tr}}\max\left(P_{batt,min} - \widetilde{P}_{em,loss} - \widetilde{P}_{batt,loss},\ P_{em,min}\right) \tag{A.52}$$

$$\widetilde{T}_{max} = \eta_{tr}\,T_{em,max} \tag{A.53}$$

$$\widetilde{T}_{min} = \frac{1}{\eta_{tr}}\,T_{em,min} \tag{A.54}$$

$$\widetilde{F}_{fri} = \begin{cases} m_{gcm}\,\dot{v}_{ref} + \widetilde{F}_r - \widetilde{F}_{long,min}, & \widetilde{F}_{long} < \widetilde{F}_{long,min} \\ 0, & \text{otherwise} \end{cases} \tag{A.55}$$

$$\widetilde{P}_{batt,loss} = \widetilde{I}_{batt}^2\,R_{batt} + \widetilde{P}_{cabHeat} \tag{A.56}$$

$$\widetilde{I}_{batt} = \frac{\widetilde{P}_{em} + \widetilde{P}_{em,loss}}{V_{batt}} \tag{A.57}$$

$$\widetilde{P}_{cabHeat} = c_{heat}\,(\widetilde{P}_{em} + \widetilde{P}_{em,loss}), \quad P_{em} > 0 \tag{A.58}$$

$$\widetilde{P}_{em,loss} = 2\,k_\omega\,\widetilde{\omega}^2 \tag{A.59}$$

$$\widetilde{\omega} = \sqrt{\frac{\widetilde{P}_{em}}{b}} \tag{A.60}$$

$$SoC_{min} \leqslant \widetilde{SoC} \leqslant SoC_{max} \tag{A.61}$$

$$\widetilde{SoC}(x) = \widetilde{SoC}(x_i) + \int_{x_i}^{x} \frac{-\widetilde{P}_{batt}}{C_{batt}} dX, \quad x_i < x \leqslant x_{i+1}, \forall\, i \in \left\{1, 2, 3\right\} \tag{A.62}$$

$$\widetilde{SoC}(x_i) = \widetilde{SoC}(x_i^-) + \frac{\widetilde{t}_{ch,i} P_{ch,i}}{C_{batt}} \tag{A.63}$$

$$\Delta\widetilde{SoC}(x_{i+1}^-) = \widetilde{SoC}(x_{i+1}^-) - \widetilde{SoC}(x_i) \tag{A.64}$$

$$\widetilde{t}_{ch,i} = \begin{cases} \min \left(\max\left(t_{lu,i},\, t_{s,i},\, \frac{[SoC_{min} - \Delta\widetilde{SoC}(x_{i+1}^-) - \widetilde{SoC}(x_i^-)]\, C_{batt}}{P_{ch,i}} \right), \right. \\ \qquad \left. \frac{[SoC_{max} - \widetilde{SoC}(x_i^-)]\, C_{batt}}{P_{ch,i}} \right), \quad P_{ch,i} > 0 \\ 0, \qquad\qquad\qquad\qquad\qquad\qquad \text{otherwise} \end{cases} \tag{A.65}$$

$$SoC_{min} \leqslant \left[\Delta\widetilde{SoC}(x_{i+1}^-) + \widetilde{SoC}(x_i^-) + \frac{\widetilde{t}_{ch,i} P_{ch,i}}{C_{batt}} \right] \leqslant SoC_{max} \tag{A.66}$$

$$\widetilde{t}_{tr} = \widetilde{t}_{tor} + \sum_{i=1}^{2} \max\left(t_{lu,i},\, \widetilde{t}_{res,i},\, \widetilde{t}_{ch,i} \right) \tag{A.67}$$

$$\widetilde{t}_{res,i} = \frac{45}{240} \frac{\widetilde{t}_{tor}}{2}, \quad i \in \left\{1, 2\right\} \tag{A.68}$$

$$\widetilde{s_h}(n_y) = 1 - \frac{n_y \widetilde{N}_t}{2 N_{cycle} C_{batt}} \int_0^{\widetilde{t}_{tr}} \left(\left| \widetilde{P}_{batt}(t) \right| + \left| \widetilde{P}_{ch}(t) \right| \right) dt \tag{A.69}$$

$$\widetilde{n}_{rep} = -\lfloor \widetilde{s_h}(n_y) \rfloor \tag{A.70}$$

$$\widetilde{R}_b = N_v\, p_{batt} \left(-\lfloor \widetilde{s_h}(n_y) \rfloor + \widetilde{s_h}(n_y) \right) (1 - d_{bp})^{n_y} \tag{A.71}$$

$$\widetilde{G}_{EV} \geqslant G_{min} \tag{A.72}$$

$$\widetilde{S}_{EV} \geqslant S_{min} \tag{A.73}$$

$$\widetilde{A}_{EV} \leqslant A_{max} \tag{A.74}$$

where a_k, $k = 1...n_{se}$ denote the design variables of n_{se} dimensional space $\boldsymbol{S}_{EV}$, in which the range of k^{th} dimension is specified by set $\boldsymbol{S}_{EV,k}$ containing discrete choices of the design variable a_k. The design variables of a battery electric vehicle include the type of electric motor, number of electric motors, type of battery pack, number of battery packs, LU of the first unit/semitrailer at the first node of the transportation task, LU of the second trailer/semitrailer (if any) at the first node of the transportation task, LU of the first unit/semitrailer at the second node, LU of the second trailer/semitrailer (if any) at the second node, and recharging power at the first and second nodes, and the ranges of these are denoted by $\boldsymbol{type}_{em}$, $\boldsymbol{N}_{em}$, $\boldsymbol{type}_{pack}$, $\boldsymbol{N}_{pack}$, $\boldsymbol{LU}_{1stTr,1}$, $\boldsymbol{LU}_{2ndTr,2}$, $\boldsymbol{LU}_{1stTr,1}$, $\boldsymbol{LU}_{2ndTr,2}$, $\boldsymbol{P}_{ch,1}$, and $\boldsymbol{P}_{ch,2}$, respectively. Several battery packs connected in series form the vehicle battery. The elements of the vehicle–related design sets are described in Table B.5. In the cost function (A.30), N_v denotes the number of vehicles, $\widetilde{f}_{tr}$ denotes the transported freight per year (described by Eq. (A.34)), and $\widetilde{c}_{elec}$ and $\widetilde{c}_{maint,ev}$ denote the annual electric energy cost and the cost of maintenance (described by Eqs. (A.31)), respectively. In Eq. (A.31), p_{el} and $\widetilde{E}_{el}$ denote the price of electric energy and the electric energy consumed during a round–trip (described by Eq. (A.40)). Eq. (A.32) is similar to Eq. (A.3). Eq. (A.33) describes the maintenance cost of a BEHV proportional to the maintenance cost of a CHV of the same size that operates in the same scenario with a proportionality factor of 50%, according to Davis and Figliozzi (2013). In Eq. (A.34), N_{em}, $m_{ElDrive}$, $N_{pack}$and m_{pack} represent the number of electric motors of the vehicle, mass of a single electric motor and its driveline, number of battery packs installed in the vehicle, and mass of a single battery pack, respectively; m_{add} denotes the additional bonus mass allowed according to EU directive 2015/719 to encourage electrified propulsion in heavy vehicles. Eq. (A.35) yields the depreciation cost of the hardware, where $\widetilde{p}_{batt,tot}$ denotes total price of initial and replaced battery packs (described by Eq. (A.38)), and vehicle–infrastructure resale value $\widetilde{R}_v$ (described by Eq. (A.37)) is different from that of the last–replaced battery $\widetilde{R}_b$ depending on its state of health. The old replaced batteries have zero resale value. The price of the vehicle–infrastructure $\widetilde{p}$ is described by Eq. (A.36), which includes the chassis price p_{chass}, price of electric motors p_{em}, transmission price p_{trans}, price of all the vehicle hardware required for ADS p_{ads}, investment cost of LU p_{lu}, investment cost of charging stations p_{rech}, and investment cost related to TMMS p_{tmms}. In Eq. (A.38), $\widetilde{n}_{rep}$ denotes the number of battery replacements during service life, p_{batt}

denotes price of the first battery at the beginning of the service life, d_{bp} represents a factor defining yearly decrease in battery price due to battery technology development and that all the batteries were bought at the beginning of the service life, and $\widetilde{n}_{yrep}$ denotes battery replacement time in years which can be calculated by solving Eq. (A.69) such that $\widetilde{s}_h(\widetilde{n}_{yrep}) = 0$. Eq. (A.39) reveals the number of trips a vehicle performs per year.

The electric energy consumed during a round–trip can be calculated using Eq. (A.40), where t_{tor} and $\widetilde{P}_{batt}$ denote the travel time on road (described by Eq. (A.41)) and the power of battery packs (described by Eq. (A.42)), respectively. In Eq. (A.41), x_f denotes the overall distance covered during the round–trip and $\widetilde{v}$ is the vehicle speed at the distance x on road (described by differential Eq. (A.48)), where $\dot{(\cdot)}$ denotes time derivative. In Eq. (A.42), $\widetilde{P}_{em}$ denotes the useful power of electric motors (described by Eq. (A.44)), $\widetilde{P}_{em,loss}$ denotes the energy loss of the electric motors (described by Eq. (A.59)), and $\widetilde{P}_{batt,loss}$ represents the energy loss of the battery packs (described by Eq. (A.56)). The power of the battery packs is constrained between the minimum and maximum values, $P_{batt,min}$ and $P_{batt,max}$, according to the constraint Eq. (A.43). In Eq. (A.44), η_{tr}, $P_{em,max}$, and $P_{em,min}$ denote the transmission efficiency and the maximum and minimum powers of electric motors, respectively. Eqs. (A.45)–(A.50) are similar to those of CHV, i.e., Eqs. (A.16)–(A.21). The maximum and minimum powers and torque on wheels, as well as the friction force, are described using Eqs. (A.51)–(A.55). In Eq. (A.56), $\widetilde{I}_{batt}$ represents the electric current in battery packs (described by Eq. (A.57)) when the battery nominal voltage V_{batt} is known, R_{batt} denotes the resistance of the battery packs and $\widetilde{P}_{cabHeat}$ the average power used in heating the driver cabin (if any) described by equation ((A.58)). The average heating power was assumed to be proportional to the consumed power by a proportionality factor c_{heat}. Eqs. (A.59) and (A.60) describe the power loss in electric motors, where k_ω denotes a constant related to electric motor specifications and ω is the rotational speed of the electric motor. This model of energy loss corresponds to electric motor operation at the highest efficiency, wherein the gearbox is capable of selecting any gear ratio that is very close to the optimum value. Such a type of transmission can be referred to as continuous variable transmission.

The state of charge (SOC) of the batteries $\widetilde{SoC}(x)$ must always be within the limits SoC_{min} and SoC_{max}, as specified by constraint Eq. (A.61). The SOC can be calculated using Eq. (A.62), wherein $\widetilde{SoC}(x_i)$ denotes the SOC at the exit of node i, x denotes the distance traveled, and C_{batt} denotes the total capacity of battery packs. The SOC at the exit of node i is given by Eq. (A.63), wherein $\widetilde{SoC}(x_i^-)$ denotes the SOC at the entrance of node i, $\widetilde{t}_{ch,i}$ is the charging time at node i, and $P_{ch,i}$ denotes the charging power at the same node. The SOC $\Delta\widetilde{SoC}(x_{i+1}^-)$ required to reach the next charging station is given by Eq. (A.64). The charging time was defined based on $\Delta\widetilde{SoC}(x_{i+1}^-)$ in accordance with Eq. (A.65) satisfying constraint (A.66).

The round–trip time $\widetilde{t}_{tr}$ can be calculated using Eq. (A.67). The resting time is given by Eq. (A.68), which is similar to the case of CHV, with the difference being that resting is possible during charging and LU. Moreover, LU takes place at the same time as charging. Eq. (A.69) describes the state of health of the battery, in accordance with the works of Wang et al. (2011), Hu et al. (2015), and Ghandriz et al. (2017), where, N_{cycle} represents the number of charge–discharge cycles before the end–of–life of the batteries. The number of battery replacements during the service life of a vehicle can be calculated using Eq. (A.70), wherein operator $\lfloor x \rfloor$ denotes the integer closest to x that is equal to or lower than x. Eq. (A.71) yields the resale value of the last–replaced battery. The resale value is zero if the state of health of the last replaced battery is zero, i.e., it reached 80% of the initial capacity. Finally, constraints (A.72)–(A.74) are similar to those of a CHV (i.e., Eqs. (A.27)–(A.29).

Owing to non–convexity and non–smoothness of the constraints, these optimization problems were solved using stochastic optimization methods, in particular particle swarm optimization, as described by Wahde (2008).

Appendix B. Parameters[2]

See Tables B.5–B.12.

Table B.5
Range of the design variables and their specification.

Design variable	Range
$\boldsymbol{type}_{ice}$	ICE_{4lit}, ICE_{6lit}, ICE_{8lit}, ICE_{11lit}, ICE_{13lit}, ICE_{16lit}
$\boldsymbol{type}_{em}$	EM_1, EM_2, EM_3
$\boldsymbol{N}_{em}$	1, 2, …, $2N^*_{axles}$
$\boldsymbol{type}_{pack}$	BP_1, BP_2
$\boldsymbol{N}_{pack}$	1, 2, …, 60
$\boldsymbol{LU}_{jthTr,i}$	OBW*, SC, AST, OBL*
$\boldsymbol{P}_{ch,i}$	10 kW, 20 kW, …, 300 kW

* N_{axles}: number of axles, OBW: on–board waiting, OBL: on–board lift.

[2] Data were acquired from Volvo Group Truck Technology.

Table B.6
Internal combustion engines.

Name	ICE_{4lit}	ICE_{6lit}	ICE_{8lit}	ICE_{11lit}	ICE_{13lit}	ICE_{16lit}
$P_{ICE,max}$ (kW)	149	234	298	410	485	550
$T_{ICE,max}$ (Nm)	900	1400	1900	2300	2600	2800
m_{ice} (kg)	400	450	500	550	600	650
$p_{ice} + p_{trans}$ (€)	11250	15000	18750	22500	26250	30000

Table B.7
ICE efficiency.

Normalized power, $\frac{P_{ice}}{P_{ice,max}}$	0.2209	0.2989	0.3768	0.4547	0.5326	0.6105	0.6884	0.7663	0.8442	0.9221	1.0000
η_{ice}	0.1995	0.3438	0.3740	0.3989	0.4101	0.4245	0.4284	0.4284	0.4318	0.4247	0.4156

Table B.8
Electric motors.

	EM_1	EM_2	EM_3
c_{em} (€)	5000	5500	8000
$T_{em,max}$ $(N.\ m)$	221	266	400
$P_{em,max}$ (kW)	107	104	70
ω_{max}, (rad/s)	1110	1047	366
$m_{ElDrive}$ (kg)	152	165	235
k_{ω}	0.0078	0.0100	0.0431
b	0.2975	0.3804	1.6362

Table B.9
Battery packs.

	$pack_1$ ⊕	$pack_2$ †
p^*_{pack} (€)	14500	10470
$P^*_{pack,min}$ (kW)	−150	−50
$P^*_{pack,max}$ (kW)	150	50
C^*_{pack} (kWh)	9.24	24.65
m^*_{pack} (kg)	200	200
V_{pack} (V)	600	600
R^*_{pack} (Ohm)	0.6	0.72
N_{cycle}	4700	2400
SoC_{max}	0.85	0.85
SoC_{min}	0.15	0.15

∗In order to get the battery parameter, this value must be multiplied by N_{pack}.
⊕ Power-optimized.
† Energy-optimized.

Table B.10
Loading–unloading schemes.

	OBL*	SC	AST	OBW*
t_{lu} (min/20ft)	20	25	15	44
p_{lu} (k€)	150	40	31	0
Additional price, container 20ft, (k€)	6	6	6	0
Additional price, container 40ft, (k€)	10	10	10	0
Additional price, ADS related sensors (k€)	0	0	10	0

* OBW: on–board waiting, OBL: on–board lift.

Table B.11
Chassis of different vehicle sizes.

	RT	TS	NC	AD
m_{gcm} (ton)	25	40	60	80
m_{chass} (ton)	9.5	15.5	24.5	32.5
m_{cab} (ton)	0.5	0.5	0.5	0.5
m_{add} (ton)	0.5	0.8	1.2	1.6
N_{axles}	3	6	8	11
R (m)	0.5	0.5	0.5	0.5
A_f (m^2)	10	10	10	10
$Ratio_{max}$	25	25	25	25
p_{chass} (k€)	90	131	166	197
p_{cab} (k€)	20	20	20	20
p_{ads}, (k€)	20	20	30	30
c_{insu}, (€/year)	2240	3000	3360	4120
c_{tax}, (€/day)	6	6	6	6

Table B.12
Other parameters and cost data.*

A_{max} (s)	29	p_d (€ $/h$)	25
c_d	0.4	p_{el} (€ $/kWh$)	0.1
c_m	0.27	p_f (€ $/lit$)	1.4
c_{heat}	0.2	p_{rech} (€ $/kW$)	1000
D_f (kg/m^3)	832	p_{trans} (€)	1500
E_{pgf} (kJ/gr)	4182.7	r	0.05
f_r	0.005	d_{bp}	0.15
g (m/s^2)	9.81	S_{min} (%)	8
G_{min} (%)	2	T_{year} (h)	8424
m_{obl} (ton)	2	η_{tr}	0.9
n_y, $(year)$	8	ρ_a (kg/m^3)	1.184

* The fuel and electric energy prices are based on Swedish market 2018.

References

Alaküla, M., Márquez-Fernández, F.J., 2017. Dynamic charging solutions in Sweden: An overview. In: Transportation Electrification Asia-Pacific (ITEC Asia-Pacific), 2017 IEEE Conference and Exp, Harbin, China. IEEE, pp. 1–6.

Alessandrini, A., Campagna, A., Delle Site, P., Filippi, F., Persia, L., 2015. Automated vehicles and the rethinking of mobility and cities. Transport. Res. Procedia 5, 145–160.

Anderson, J.M., Nidhi, K., Stanley, K.D., Sorensen, P., Samaras, C., Oluwatola, O.A., 2014. Autonomous Vehicle Technology: A Guide for Policymakers. Rand Corporation, Santa Monica, California.

Botsford, C., Szczepanek, A., 2009. Fast charging vs. slow charging: Pros and cons for the new age of electric vehicles. In: International Battery Hybrid Fuel Cell Electric Vehicle Symposium, Stavanger, Norway.

Brown, A., Gonder, J., Repac, B., 2014. An analysis of possible energy impacts of automated vehicles. In: Road Vehicle Automation. Springer, Cham, pp. 137–153.

Chan, C.-Y., 2017. Advancements, prospects, and impacts of automated driving systems. Int. J. Transport. Sci. Technol. 6 (3), 208–216.

Davis, B.A., Figliozzi, M.A., 2013. A methodology to evaluate the competitiveness of electric delivery trucks. Transport. Res. Part E: Logist. Transport. Rev. 49 (1), 8–23.

Edgar, J., Prem, H., Calvert, F., 2002. Applying performance standards to the Australian heavy vehicle fleet. In: Proceedings of the 7th International Symposium on Heavy Vehicle Weights & Dimensions, Delft, The Netherlands, pp. 73–96.

Edlund, S., Fryk, P.-O., 2004. The right truck for the job with global truck application descriptions. Technical report, SAE technical paper.

European Commission, 2016. Road transport: Reducing CO_2 emissions from vehicles. Technical report.

Feng, W., Figliozzi, M., 2013. An economic and technological analysis of the key factors affecting the competitiveness of electric commercial vehicles: A case study from the USA market. Transport. Res. Part C: Emerg. Technol. 26, 135–145.

Flämig, H., 2016. Autonomous vehicles and autonomous driving in freight transport. In: Autonomous Driving. Springer, Berlin, Heidelberg, pp. 365–385.

Fyhr, P., Domingues, G., Andersson, M., Márquez-Fernández, F.J., Bängtsson, H., Alaküla, M., 2017. Electric roads: Reducing the societal cost of automotive electrification. In: Transportation Electrification Conference and Expo (ITEC), 2017 IEEE, Chicago, IL, USA. IEEE, pp. 773–778.

Ghandriz, T., Hellgren, J., Islam, M., Laine, L., Jacobson, B., 2016. Optimization based design of heterogeneous truck fleet and electric propulsion. In: 2016 IEEE 19th International Conference on, Rio de Janeiro, Brazil Intelligent Transportation Systems (ITSC). IEEE, pp. 328–335.

Ghandriz, T., Jacobson, B., Laine, L., Hellgren, J., 2020. Optimization data on total cost of ownership for conventional and battery electric heavy vehicles driven by human and by automated driving systems. Data in brief (in press).

Ghandriz, T., Laine, L., Hellgren, J., Jacobson, B., 2017. Sensitivity analysis of optimal energy management in plug-in hybrid heavy vehicles. In: Intelligent Transportation Engineering (ICITE), 2017 2nd IEEE International Conference on, Singapore, Singapore. IEEE, pp. 320–327.

Hagman, J., Ritzén, S., Stier, J.J., Susilo, Y., 2016. Total cost of ownership and its potential implications for battery electric vehicle diffusion. Res. Transport. Bus. Manage. 18, 11–17.

Harper, C.D., Hendrickson, C.T., Samaras, C., 2016. Cost and benefit estimates of partially-automated vehicle collision avoidance technologies. Accident Analysis & Prevention 95, 104–115.

Hovgard, M., Jonsson, O., Murgovski, N., Sanfridson, M., Fredriksson, J., 2018. Cooperative energy management of electrified vehicles on hilly roads. Control Eng. Practice 73, 66–78.
Hu, X., Johannesson, L., Murgovski, N., Egardt, B., 2015. Longevity-conscious dimensioning and power management of the hybrid energy storage system in a fuel cell hybrid electric bus. Appl. Energy 137, 913–924.
Johannesson, L., Murgovski, N., Jonasson, E., Hellgren, J., Egardt, B., 2015. Predictive energy management of hybrid long-haul trucks. Control Eng. Practice 41, 83–97.
Johannesson, P., Podgórski, K., Rychlik, I., Shariati, N., 2016. AR (1) time series with autoregressive gamma variance for road topography modeling. Probab. Eng. Mech. 43, 106–116.
Kalra, N., Paddock, S.M., 2016. Driving to safety: How many miles of driving would it take to demonstrate autonomous vehicle reliability? Transport. Res. Part A: Policy Practice 94, 182–193.
Khan, A., Harper, C.D., Hendrickson, C.T., Samaras, C., 2019. Net-societal and net-private benefits of some existing vehicle crash avoidance technologies. Accident Anal. Prevent. 125, 207–216.
Kharrazi, S., Karlsson, R., Sandin, J., Aurell, J., 2015. Performance based standards for high capacity transports in Sweden, FIFFI project 2013-03881, report 1: Review of existing regulations and literature.
Kopfer, H., Vornhusen, B., 2017. Energy vehicle routing problem for differently sized and powered vehicles. J. Bus. Econ. 1–29.
Lebeau, P., Macharis, C., Van Mierlo, J., 2019. How to improve the total cost of ownership of electric vehicles: An analysis of the light commercial vehicle segment. World Electric Vehicle Journal 10 (4), 90.
Lebeau, P., Macharis, C., Van Mierlo, J., Lebeau, K., 2015. Electrifying light commercial vehicles for city logistics? A total cost of ownership analysis. Eur. J. Transport Infrastruct. Res. 15 (4).
Lee, D.-Y., Thomas, V.M., Brown, M.A., 2013. Electric urban delivery trucks: Energy use, greenhouse gas emissions, and cost-effectiveness. Environ. Sci. Technol. 47 (14), 8022–8030.
Levin, M.W., Boyles, S.D., 2015. Effects of autonomous vehicle ownership on trip, mode, and route choice. Transp. Res. Rec. 2493 (1), 29–38.
Liu, C.-I., Jula, H., Vukadinovic, K., Ioannou, P., 2004. Automated guided vehicle system for two container yard layouts. Transport. Res. Part C: Emerg. Technol. 12 (5), 349–368.
Maurer, M., Gerdes, J.C., Lenz, B., Winner, H., et al., 2016. Autonomous Driving, vol. 10 Springer Berlin Heidelberg, Berlin, Germany.
Mersky, A.C., Samaras, C., 2016. Fuel economy testing of autonomous vehicles. Transpor. Res. Part C: Emerg. Technol. 65, 31–48.
Milanes, V., Villagra, J., Godoy, J., Simo, J., Pérez, J., Onieva, E., 2012. An intelligent v2i-based traffic management system. IEEE Trans. Intell. Transp. Syst. 13 (1), 49–58.
Nesterova, N., Quak, H., Balm, S., Roche-Ceraso, I., Tretvik, T., 2013. State of the art of the electric freight vehicles implementation in city logistics. FREVUE Project Deliverable D, 1.
Nowakowski, C., Shladover, S.E., Tan, H.-S., 2015. Heavy vehicle automation: Human factors lessons learned. Procedia Manuf. 3, 2945–2952.
Palmer, K., Tate, J.E., Wadud, Z., Nellthorp, J., 2018. Total cost of ownership and market share for hybrid and electric vehicles in the UK, US and Japan. Appl. Energy 209, 108–119.
Pelletier, S., Jabali, O., Laporte, G., 2016. 50th anniversary invited article—goods distribution with electric vehicles: review and research perspectives. Transport. Sci. 50 (1), 3–22.
Pettersson, P., Berglund, S., Ryberg, H., Jacobson, B., Karlsson, G., Brusved, L., Bjernetun, J., 2018. Comparison of dual and single clutch transmission based on global transport application mission profiles. Int. J. Veh. Des. 77 (1–2), 22–42.
Pettersson, P., Jacobsson, B., Johannesson, P., Berglund, S., Laine, L., 2016. Influence of hill-length on energy consumption for hybridized heavy transports in long-haul transports. In: 7th Commercial Vehicle Workshop, 13 May 2016. Graz, Austria.
Sadeghi Kati, M., 2013. Definitions of performance based characteristics for long heavy vehicle combinations. Technical report.
Sadeghi Kati, M., Fredriksson, J., Laine, L., Jacobson, B., 2014. Evaluation of dynamical behaviour of long heavy vehicles using performance based characterstics. In: FISITA 2014 World Automotive Congress-2-6 June 2014, Maastricht, The Netherlands.
SAE standard, 2016. Taxonomy and definitions for terms related to on-road motor vehicle automated driving systems. SAE Standard J. 3016, 1–16.
Taefi, T.T., Kreutzfeldt, J., Held, T., Fink, A., 2015. Strategies to increase the profitability of electric vehicles in urban freight transport. In: E-Mobility in Europe. Springer, Cham, pp. 367–388.
Taefi, T.T., Kreutzfeldt, J., Held, T., Fink, A., 2016a. Supporting the adoption of electric vehicles in urban road freight transport–a multi-criteria analysis of policy measures in Germany. Transport. Res. Part A: Policy Practice 91, 61–79.
Taefi, T.T., Kreutzfeldt, J., Held, T., Konings, R., Kotter, R., Lilley, S., Baster, H., Green, N., Laugesen, M.S., Jacobsson, S., et al., 2016b. Comparative analysis of European examples of freight electric vehicles schemes—a systematic case study approach with examples from Denmark, Germany, the Netherlands, Sweden and the UK. In: Dynamics in Logistics. Springer, Cham, pp. 495–504.
Taefi, T.T., Stütz, S., Fink, A., 2017. Assessing the cost-optimal mileage of medium-duty electric vehicles with a numeric simulation approach. Transport. Res. Part D: Transport Environ. 56, 271–285.
Taiebat, M., Brown, A.L., Safford, H.R., Qu, S., Xu, M., 2018. A review on energy, environmental, and sustainability implications of connected and automated vehicles. Environ. Sci. Technol. 52 (20), 11449–11465.
Torabi, S., Wahde, M., 2018. Fuel-efficient driving strategies for heavy-duty vehicles: A platooning approach based on speed profile optimization. J. Adv. Transport., 2018.
Tsugawa, S., Jeschke, S., Shladover, S.E., 2016. A review of truck platooning projects for energy savings. IEEE Trans. Intell. Vehicles 1 (1), 68–77.
Ullrich, G., 2015. Automated Guided Vehicle Systems. Springer-Verlag, Berlin.
Wadud, Z., 2017. Fully automated vehicles: A cost of ownership analysis to inform early adoption. Transport. Res. Part A: Policy Practice 101, 163–176.
Wadud, Z., MacKenzie, D., Leiby, P., 2016. Help or hindrance? the travel, energy and carbon impacts of highly automated vehicles. Transport. Res. Part A: Policy Practice 86, 1–18.
Wahde, M., 2008. Biologically Inspired Optimization Methods: An Introduction. WIT Press, Southampton.
Wang, J., Liu, P., Hicks-Garner, J., Sherman, E., Soukiazian, S., Verbrugge, M., Tataria, H., Musser, J., Finamore, P., 2011. Cycle-life model for graphite-lifepo4 cells. J. Power Sources 196 (8), 3942–3948.
Wu, G., Inderbitzin, A., Bening, C., 2015. Total cost of ownership of electric vehicles compared to conventional vehicles: A probabilistic analysis and projection across market segments. Energy Policy 80, 196–214.